Life Sciences 239 (2019) 116870

Contents lists available at ScienceDirect

Life Sciences

journal homepage: www.elsevier.com/locate/lifescie

Review article

Recent developments in peptide-based SPECT radiopharmaceuticals for breast tumor targeting

Sajjad Ahmadpour[a], Seyed Jalal Hosseinimehr[b,*]

[a] Pharmaceutical Sciences Research Center, School of Pharmacy, Ardabil University of Medical Sciences, Ardabil, Iran
[b] Department of Radiopharmacy, Faculty of Pharmacy, Mazandaran University of Medical Sciences, Sari, Iran

ARTICLE INFO

Keywords:
Breast cancer
SPECT
Radiolabeled peptide
Targeting
Diagnosis

ABSTRACT

Breast cancer deaths occur mainly because of poor diagnosis in early stages that lead to tumor metastasis in advanced stages. Developing a high-sensitive early-stage breast cancer diagnostic tool based on single photon emission computer tomography (SPECT) and positron emission tomography (PET) are urgent. There are several evidences to demonstrate the prominent roles of specific receptors overexpression in tumor initiation and progression of breast cancer. Targeting of specific receptor with radiolabeled biomolecule is a suitable tool for early diagnosis of breast cancer. In recent years, investigators have paid their attention in the development of peptide-based radiopharmaceuticals due to their favorable pharmacokinetics that offer diagnostic applications for breast cancer imaging. Various characterizing techniques permit the preparation of variety of peptides that allow efficiently labeling with clinically useful SPECT radionuclides such as ^{99m}Tc, ^{123}I and ^{111}In without compromising biological properties. In this review, we focus on the recent developments in use of peptide-based SPECT radiopharmaceuticals for breast cancer targeting and imaging.

1. Introduction

Breast cancer is the most common type of cancer in the entire world and comprises 18% of all female cancers [1]. Breast cancer is numerate highly heterogeneous tumor and mainly is categorized into four different subtypes: luminal A, luminal B, HER2-positive and triple-negative [2–5]. The main risk factors for breast cancer are including environmental, reproductive, and lifestyle factors and less than 10% of breast cancers can be attributed to an inherited genetic mutation [6]. In majority of breast cancer patients, death is caused by metastasis especially brain metastasis and often their treatment is hampered because of low treatment response rate [6]. For breast cancer patients without any site of a tumor metastasis, the 5-year survival rate is 99%, whereas when metastasis has been occurred, the survival rate significantly reduces to 26% (2016). As there are few signs and symptoms early on, precise diagnosis of breast cancer via sensitive molecular probes is very important in reducing mortality of breast cancer. One of the most sensitive techniques that has been utilized in the early diagnosis of breast cancer is molecular imaging with single photon emission computed tomography (SPECT) or positron-emission tomography (PET). Molecular imaging as compared with other imaging modalities such as computed tomography (CT), Magnetic Resonance Imaging (MRI), mammography and ultrasound, provides benefit information about both morphological or structure and function information such as perfusion, tissue metabolism and specially receptor density. The utilization of hybrid system such as SPECT/CT or PET/CT, provides a rapid whole-body imaging with high diagnostic accuracy. In other words, the fusing of CT or MRI with PET or SPECT provides the precise anatomical localization of radionuclide for attenuation correction and permits uptake value which can be correctly quantified by SPECT/CT or PET/CT, that it is provided supplementary information on breast cancer. These hybrid techniques improve the sensitivity of diagnosis at early stage for good decision in effective therapy planning. SPECT imaging can easily diagnose bone metastasis of breast cancer with high sensitivity and specificity [7,8]. For vertebral metastasis, SPECT imaging is superior to MRI in detecting extra-vertebral body metastasis [9]. With respect to the ability of SPECT imaging in many patients, may be need to correlation with high-quality anatomic images, CT, or MRI. Therefor it's better that Hybrid SPECT/CT devices equipped with multislice CT scanners were used [10]. It has been demonstrated various types of receptor such as, HER2 [11], EGFR [12], hepatocyte growth factor receptor (HGFR; also known as c-MET), type I insulin-like growth factor receptor (IGFIR) and estrogen receptor (ER) [13] that are overexpressed on breast cancer cells that regulate important biological processes, including cell proliferation, differentiation, metabolism, and survival with different signaling pathways. These receptors provide unique

* Corresponding author.
E-mail addresses: sjhosseinim@yahoo.com, sjhosseinim@mazums.ac.ir (S.J. Hosseinimehr).

https://doi.org/10.1016/j.lfs.2019.116870
Received 11 August 2019; Received in revised form 9 September 2019; Accepted 10 September 2019
Available online 13 September 2019
0024-3205/

characteristics for cancerous cells that are attractions as specific targets for imaging and therapy of cancers [14–17]. Receptor-binding radiolabeled peptides are precise probes for early detection of breast cancer due to the targeting of ligand-binding extracellular domains of these mentioned receptors [18–23]. This review outlines the potential applications of peptide-based radiopharmaceuticals for breast cancer diagnosis and provides future research perspective in this field.

1.1. Targets on breast cancer cells for imaging

Targeting of molecular marker overexpressed on breast cancer cells with a radiotracer can be served as a sensitive and specific tool for early diagnosis and consequently effective therapy. According to the progression of cancer cells, the amplification and overexpression of tumor specific receptors lead to the increased relapse rates and decreased survival rate. There is several evidences to demonstrate various type of receptors be expressed in breast cancer for initiation and progression [11,12]. The crucial information of receptor overexpression on tumor can be gained using the specific targeting radiotracer. A good lesion visualization is related to the type/subtype and density of an overexpressed receptor in cancer cell. Meanwhile, molecular imaging agent which is selected for lesion visualization, should be chosen carefully. So far, several main receptors such as estrogen receptor (ER), progesterone receptor (PR), human epidermal growth factor receptor 2 (HER2), epidermal growth factor receptor (EGFR), somatostatin receptor (SSTR), and the bombesin receptor (BR) are being identified and investigated for tumor targeting (Fig. 1). HER2 and EGFR receptors are belonging to tyrosine kinase receptors and numerated as two main overexpressed receptors in breast cancer. Tyrosine kinase receptors has important role in biological processes, including cell survival, proliferation, differentiation, motility, apoptosis, survival, invasion, migration, adhesion, and angiogenesis [24–27]. So far, 58 members of the tyrosine kinase family identified that further are divided into 20 subfamilies [27,28]. Much evidences are coming that dysregulation of these receptors lead to the development of cancers [29,30]. It is demonstrated that 25–30% patients with primary breast cancer overexpress HER2 receptor and are associated with poor clinical outcome and cancer progression [27,31]. Trastuzumab, as a monoclonal antibody, was the first targeted therapy approved by the FDA for breast cancer with overexpressed HER2 receptor [32], however several FDA approved HER2-targeted drugs are in clinical trials [33–35]. EGFR overexpression in breast cancer was observed in 15–30% of patients with large tumor size and poor clinical outcomes [36–39]. EGFR overexpress is associate with poor prognosis in triple-negative breast cancer and attributed to EGFR gene amplification [40–44]. In contrast to other EGFR related cancers such as lung cancer, the mutation of EGFR in breast cancer is rare [40]. Breast cancer is classified into three subtypes with consideration the level of hormone receptor (HR) and HER2 protein including, estrogen receptor (ER)-/progesterone receptor (PR) - positive type (~70–75%), (2) triple-negative type (10–15%), and (3) HER2 positive type (~5%). Estrogen receptor positive (ER+) tumors are the most common form of breast cancer in patients. Unlike triple-negative breast cancer (TNBC) that do not have well-defined molecular targeted drugs [45], in the case of estrogen and progesterone receptors (ER and PR) positive patient's estrogen deprivation has become an essential treatment for HR + breast cancer with decreasing the activation of the ER mediated signaling and avoiding cancer cell proliferation [46,47]. Somatostatin receptors (SSTRs) are belonging to a family of G-protein-coupled receptors (GPCRs) that have five known subtypes (numbered 1–5), overexpressed in various type of cancers such as lung, prostate and neuroendocrine breast cancer (NEBC) as well as no special type (NST) breast cancer [48,49]. The expression of SSTR in breast cancer can be related to hormone receptor expression, lymph node involvement, postmenopausal status and tumor stage. SSTR2A is being associated with the strongest anti-proliferative effect and is the subtype with high overexpression in NST. NEBC is a group of rare tumors with variant incidence between 0.1% and 18%, with three subtypes including, poorly differentiated small cell carcinoma, well-differentiated carcinoma and invasive breast carcinoma. However, NST invasive breast cancer is most common. Due to the overexpression of SSTRs in breast cancer, radiolabeled somatostatin analogues can be served as a successful probe for visualizing primary and metastatic breast cancer [50,51]. The gastrin-releasing peptide (bombesin) receptor (GRP-r) is belonging to a family of G-protein-coupled receptors (GPCRs) that is overexpressed in some cancers such as GRP-r-positive prostate tumor and breast cancer [52]. It is demonstrated that GRP-r plays a critical role in the initiation and progression of breast cancer. In breast cancer cells, one or more than one of the three known GRPs receptors may be expressed. Bombesin is a tetradecapeptide that binds to the GRP-r. So far, various radiolabeled analogues of this peptide have

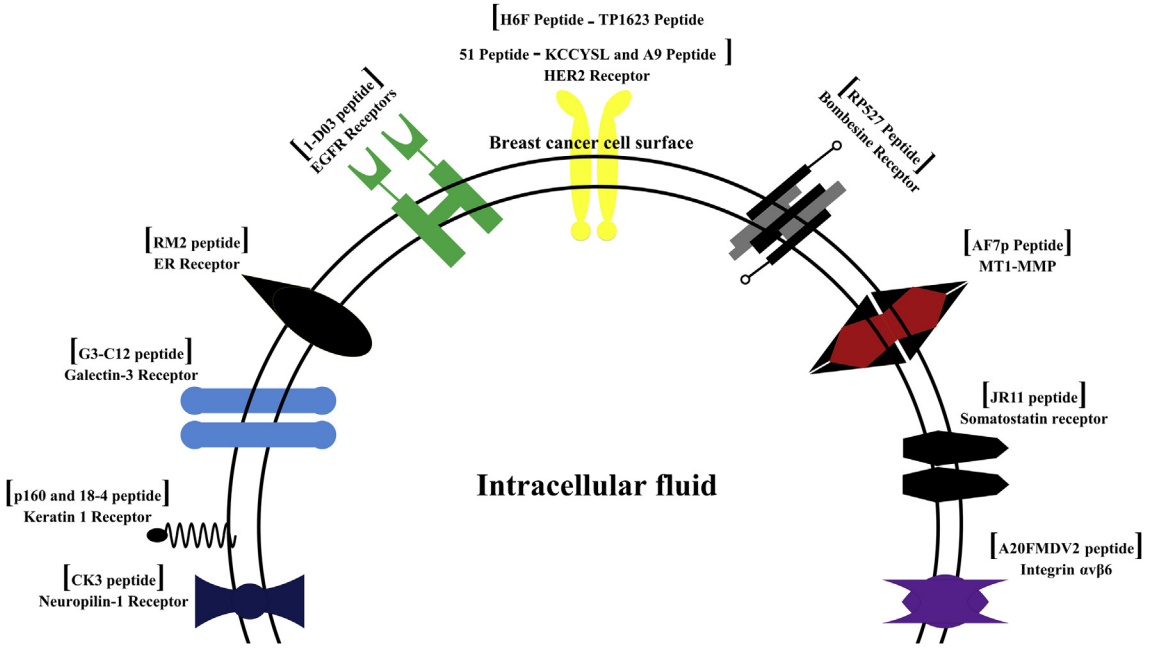

Fig. 1. The schematic design of various types of targets overexpressed in breast cancer cell surface and related peptides for these targets for breast cancer targeting.

been developed for imaging of breast cancer [53].

Targeting of these receptors with high affinity probes may lead to early diagnosis of breast cancer and subsequently lead to effective therapy. Therefore, seeking and radiolabeling of new high affinity ligands for targeting of tumor specific receptors which are overexpressed in tumor cells are currently under investigation.

1.2. Radiolabeled peptides for breast cancer targeting and imaging

Molecular imaging represents promising target for early diagnosis and effective therapy of cancer. Diagnosis and therapy using radiolabeled biomolecules including peptide [54,55], antibody [56], aptamer [57–60] and small molecule [61,62] have been successfully applied for breast cancer with specific receptor overexpression. In comparison to proteins and antibodies, small peptides are currently the agents of choice for molecular imaging and therapy of cancers due to favorable pharmacokinetic characteristics are including small size, easy preparation and radiolabeling with various methods, high resistance to radiolabeling condition, rapid wash out from blood circulation, low toxicity and high ratio of tumor to non-tumor tissue and affinity [63–65]. However, among these characterizations, high binding affinity and especially good receptor-mediated internalization are critical parameters for imaging and therapy. As mention above, tumor cells possess receptors on their surfaces that can be used for diagnostic and therapeutic aims during labelling with various radionuclides such as ^{99m}Tc, ^{123}I, ^{111}In and ^{18}F [66]. In the past years a number of molecular targets for receptor targeted nuclear imaging of breast cancer [67] and also specific analogues such as somatostatin analogues (SST receptor) [68], vasoactive intestinal peptide (VIP) [69] (VPAC Receptors), Affibody [70–73] (EGF Receptor), RGD [74] (Integrins receptor), bombesin analogues [75] (GRPs receptors) and alpha-melanocyte stimulating hormone peptide analogues [76] (Melanocortin, MC receptors) have been identified and are currently under investigation. One of the main pitfall related to imaging with radiolabeled peptide is short plasma half-life, which is usually due to fast degradation in plasma by peptidases and proteases and/or washout [77,78]. So far, various methods have been developed to inhibition of proteolysis of native peptides to use as clinically agents [65,77,79]. In nuclear medicine practice, two main methods including SPECT and PET have been described for detection, staging and monitoring of breast cancer lesions. However, PET technique has an advantage over SPECT in the resolution, but SPECT technique exhibiting comparable sensitivity and leads to produce radiopharmaceuticals at a reasonable price as well as accessible [80,81]. As respect to that, ^{99m}Tc radionuclide has excellent characteristics such as easy availability from ^{99}Mo/^{99m}Tc generator, suitable photonic characteristics and dosimetry, in nuclear medicine, and is used for medical imaging in 80% of cases all over the world [82–85]. Several radiotracers such as ^{18}F-FDG PET [86–88], and ^{99m}Tc-MIBI [89–91] or ^{201}Tl-scintigraphy [92,93] have been used for breast cancer targeting. However, these radiotracers are not tumor specific and accumulate in highly proliferative tissue. Owing to the fact that targeting of tumor specific receptor with radiolabeled peptide is specific process and is mainly mediated with overexpressed receptors in cancer cells, radiolabeled peptide for breast cancer targeting has superiority to these radiotracers. The characterizations of radiolabeled peptides are summarized in Table 1 with more details.

1.3. ^{99m}Tc-HYNIC-H6F peptide

Two peptides YLFFVFER (H6) and KLRLEWNR (H10) with specific targeting on human epidermal growth factor receptor 2 (HER2) were identified via screening strategy based on *in situ* single bead sequencing on a microarray [94]. Fluorescein 5-isothiocyanate (FITC) labeled peptide H6 (FITC-H6) and H10 (FITC-H10) showed high signal on the membrane for HER2 high-expressing human breast cancer cell line SKBR-3. The K_D values of H6 and H10, which were obtained via surface plasmon resonance imaging (SPRi), were equal to 67 and 30 nM, respectively. These peptides showed low cytotoxicity at concentrations ranging from 0.1 μM to 100 μM. The results of labeled H6 and H10 peptides with CdSe QDs into SKBR-3 xenograft mice, after half an hour postinjection, showed that the peptide-QDs uptakes were observed in tumor in a specific manner. However, the tumor site with H6-QDs displayed a higher signal than H10-QDs. Pharmacokinetic result demonstrated that H10 peptide was cleared more rapidly than H6 peptide in the blood circulation (17 min for H6 v.s 13 min for H10). These results revealed that although the dissociation constants of both eptides were close to each other, the specificity of H6 was better than H10 on HER2. With view to this characterization, Li et al. aimed to develop ^{99m}Tc-HYNIC-H6F as a SPECT imaging probe for breast cancer imaging [95]. They conjugated H6F (YLFFVFER) peptide with the bifunctional chelator hydrazinonicotinamide (HYNIC) and efficiently labeled in the presence of tricine/trisodium triphenylphosphine-3, 3′, 3″-trisulfonate (TPPTS) as the co-ligand with ^{99m}Tc radionuclide. ^{99m}Tc-HYNIC-H6F had excellent *in vitro* stability in saline for 6 h. The close IC_{50} (50% inhibitory concentrations) values for HYNIC–H6F (11.25 ± 2.14 nM) and H6F (7.48 ± 3.26 nM) to HER2-positive MDA-MB-453 cells demonstrated that the conjugation of HYNIC had little impact on ligand-receptor binding affinity. The biodistribution results for ^{99m}Tc-HYNIC-H6F in nude mice bearing MDA-MB453 (HER2 positive cell line) and MDA-MB-231(HER2 negative cell line) tumors at 30 min showed the uptake of ^{99m}Tc-HYNIC-H6F was significantly higher in MDA-MB-453 tumors than in MDA-MB-231 tumors (2.47 ± 0.12 v.s 0.99 ± 0.19 % ID/g). These results were agreement with flow cytometry studies about this peptide and confirming that the HER2 protein is a specific target for H6F peptide. The highest tumor-to-organ ratio was reported at 1 h postinjection (p.i) for ^{99m}Tc-HYNIC-H6F. SPECT/CT imaging visualized the MDA-MB-453 tumors (< 5 mm in diameter) as early as 30 min p.i. with high contrast compared with the contralateral background. This tumor uptake was specific and co-injection of an excess dose of cold H6F peptide with ^{99m}Tc-HYNIC-H6F was resulted in significant reduced tumor uptake at 30 min p.i. (from 2.47 ± 0.12 to 1.03 ± 0.37 %ID/g). Because of HER2 protein overexpressed in patients with newly diagnosed primary invasive breast cancer [96] and with respect to that HER2 protein is the specific target of the H6F peptide, ^{99m}Tc-HYNIC-H6F has potential clinical application for whole-body screening of HER2-positive metastatic tumors. This ability is related to the favorable *in vitro* and *in vivo* stability and high affinity in the range of nM toward HER2 receptor, confirmed by high *in vivo* tumor uptake for MDA-MB-453 tumors (HER2 +) than in MDA-MB-231 tumors (HER2$^-$). The *in vivo* tumor uptake are mainly mediated by HER2 receptors could effectively detect HER2-positive breast cancers with high tumor-to-muscle ratios. Fast wash out of ^{99m}Tc-HYNIC-H6F from blood circulation caused low uptake in non-target organs, low burden excess radiation in patients and especially high tumor contrast for tumors that are in the near of heart and lungs. Therewith, fast tumor uptake for ^{99m}Tc-HYNIC-H6F leads to low waiting time between administrations and imaging. The attachment of H6F peptide to HYNIC chelator not only didn't decrease the binding affinity to the specific targets, but also assembled the convenient formulation of a labeling kit with popular ^{99m}Tc. Trastuzumab is approved for first-line treatment of HER2-positive breast cancer, but trastuzumab monotherapy response rate for metastatic breast cancer is less than 34% [97,98] and in about one third of patients during trastuzumab-based neoadjuvant therapy, HER2-positive breast cancer tumors converted to HER2-negetive [99]. Therefore, monitoring the response to therapies for precision medicine in HER2 positive breast cancer patients is very important. The particular characterization for H6F peptide is the different binding domain from trastuzumab without any competition for binding during therapy. This ability for H6F peptide not only facilitates HER2-targeted therapy but also effectively monitors the efficacy of trastuzumab by rechecking the expression level of HER2 without blocking effect during therapy.

Table 1
Peptide-based radiopharmaceuticals for breast cancer imaging.

Peptide name and sequence	BFCA and radionuclide	Results	Ref.
H6F (YLFFVFER)	^{99m}Tc-HYNIC-H6F with 92.6% radiochemical purity	i *In vitro* stability in saline for 6 h ii IC_{50} = 11.25 ± 2.14 nM for MDA-MB-453 HER2 positive breast tumor cells iii Specific *in vivo* tumor uptake for MDA-MB-453 tumors (2.47 ± 0.12 %ID/g) in comparison to MDA-MB-231 tumors (0.99 ± 0.19 %ID/g) iv Main exerted way from kidneys v Highest tumor-to-organ ratio at 1 h vi High contrast MDA-MB-453 tumor visualization after 30 min	[94,95]
αM_2 (YCAREPPTRTFAYWG)	Direct radiolabeling via ^{99m}Tc with > 90% radiochemical purity	i *In vitro* stability (> 85%) after 24 h ii Significantly lower affinity in comparison to parent antibody iii Favorable kinetics with rapid excretion in women with breast cancer iv Tumor/non-tumor value between 2-4 in patients without any toxic or adverse reaction	[96,97]
MAG_3-PPP-aM2 (PPP-YAAREPPTRTFAYWG)	Cysteine residue in αM_2 peptide replace with alanine in position 2 and tri pro residue as spacer and radiolabeled via ^{99m}Tc with high radiochemical purity (> 95%)	i *In vitro* stability (> 90%) after 24 h at room temperature ii High *in vitro* serum stability equal to 80% after 4 h incubation at 37 °C. iii Slightly high lipophilicity than αM_2 iv ^{99m}Tc-MAG_3-αM_2 has a relatively higher cellular uptake than ^{99m}Tc-aM_2 for human breast cancer cells (MCF-7 and MDA-MB-231) v Maximum internalization for MCF-7 cells after 60 min incubation vi ^{99m}Tc-MAG_3-αM_2 has a faster blood clearance and superior urinary excretion properties than ^{99m}Tc-αM2 vii ^{99m}Tc-MAG_3-αM_2 has considerably lower kidneys uptake than ^{99m}Tc-αM2 viii ^{99m}Tc-MAG_3-αM_2 and ^{99m}Tc-αM2 have similar tumor uptake	[96]
FAPVLDGAVSTLLGV or (peptide A) for targeting the PTCH receptor on breast cancer cells	Radiolabeling with ^{99m}Tc in the presence of N, N'-ethylene-di-*L*-cysteine (EC) chelator with using lysine residue as linker and high radiochemical purity (> 95%)	i *In vitro* cellular uptake for three breast cancer cell lines, SUM159, MDA-IBC3, and 13762 and the highest radiotracer uptake (at 4 h) for SUM159 cell line ii Good tumor uptake up to 4 h after injection for all breast cancer cell lines, SUM159, MDA-IBC3, and 13762 according to scintigraphy results iii Good tumor visualization due to the average tumor-to-muscle ratio of 4.5 at 1 h for all breast cancer cell lines, SUM159, MDA-IBC3, and 13762	[98–100]
TP1623 peptide or (G (D) AGG-Aba YCFPDEEGACY-NH2	Radiolabeling with ^{99m}Tc radionuclide without isolation and purification	i *In vitro* stability (93.2%) after 6 h at room temperature and good serum stability up to 86% after 24h incubation with human serum ii Receptor mediated tumor uptake for SKBR3 human breast cancer iii Fast urinary excretion in normal mice lead to reduction of radioactivity in blood circulation after 120 min iv High *in vivo* stability according to the results of scintigraphy in SKBR3 human breast cancer v Good and specific visualization at 30 min (T/NT was 2.19) that reaches the peak at 120 min (T/NT was 5.18) with low blood-pool background in a short time due to fast urinary excretion	[101–103]
KCCYSL peptide	Radiolabeling with ^{111}In to develop ^{111}In-DOTA(Gly-Ser-Gly)-KCCYSL with high radiochemical purity after purification with RP-HPLC	i *In vitro* stability after 6 h incubation with phosphate buffer saline ii High *in vitro* mouse serum stability up to 60 min incubation at 37 °C iii Receptor-binding mediated uptake to MDA-MB-435(HER2 positive) human breast carcinoma cells and reach to maximum after 2h and minimal binding to K-562 human chronic myeloid leukemia cells (HER2 negative) iv IC_{50} = 42.5 ± 2.76 nM for MDA-MBA-435 breast carcinoma cells v Internalization equal to 11% of the total bound radioactivity after 2 h incubation for MDAMB-435 carcinoma cells vi Maximum normal organ uptake for kidneys due to the primary route of excretion vii Tumor-to-blood ratio of 5.0 at the end of 2 h, and 0.67 after 15 min for MDAMB-435 carcinoma cells viii Good ability for MDAMB-435 tumor visualization at 2 h	[104]
1-D03 (MEGPSKCCYSLALSH)			[105]

(*continued on next page*)

Table 1 (*continued*)

Peptide name and sequence	BFCA and radionuclide	Results	Ref.
	Radiolabeled with ^{111}In with high radiochemical purity (> 95%)	i Stability in buffer and mouse serum was greater than 24 h ii IC_{50} = 289 ± 13 nM for MDA-MBA-435 breast carcinoma cells iii ^{111}In-DOTA-1-D03 showed higher binding and specificity (specificity ratio of 7.44) for MDA-MB-435 than KCCYSL iv Maximum tumor to blood ratio (6.02 ± 0.13) after 2 h v Low kidney retention than KCCYSL at 2 h vi Good ability for MDAMB-435 tumor visualization after 2 h	
Peptide 51(ATWLPVPVVGYFMASA)	Conjugated to (DOTA) at N-terminal with GSG spacer and radiolabeled with ^{111}In radionuclide	i IC_{50} = 16 ± 7 nM for BT-474 human breast cancer cells ii Tumor uptake equal to 0.12 ± 0.02 %ID/g after 2 h iii Tumor to blood ratio and tumor to muscle ratio equal to 2.3 and 7.1 respectively iv Good ability for BT-474 human breast tumor visualization after 2 h	[106]
G3-C12 peptide (ANTPCGPYTHDCPVKR)	Conjugated to (DOTA) via Gly-Ser-Gly (GSG)–linker and radiolabeled with ^{111}In radionuclide with more than 98% radiochemical purity after purification by C18 RP-HPLC	i Stability in phosphate-buffered saline (PBS) was greater than 98% after 12 h and for serum (85%) and urine (80%) at 30 min ii Specific binding for galectin-3 positive MDA-MB-435 human breast cancer cells and negligible binding to BT549 (galectin-3 negative) breast carcinoma cells iii Cell surface binding without internalization iv IC_{50} value = 200 nM for MDA-MB-435 human breast cancer cells v Rapid and specific tumor uptake and blood clearance kinetics in MDA-MB-435 human breast cancer xenografts vi Tumor-to-blood ratio of 8.6 at 2 h vii Good ability for MDAMB-435 tumor visualization at 2 h with high tumor-to-background contrast	[107]
AF7p (His-Trp-Lys(Dde)-His-Leu-His-Asn-Thr-Lys(Dde)-Thr-Phe-Leu)	Radiolabeling with ^{99m}Tc in the presence of HYNIC chelator and (Tricine/TPPTS) coligand and high radiochemical purity (> 95%) after purification	i Stability in normal saline 93% during the 6 h' incubation and 94% in the solution containing excess cysteine during the 6 h' incubation ii Specific binding to MDA-MB-231(MT1-MMP positive) human breast carcinoma cells and insignificant binding to A549 cell which low expresses of MT1-MMP iii Mainly excreted through the renal-urinary routes iv Tumor-to-Muscle (4.17) and Tumor-to-Blood (11.11) at 2 h post-injection for MDA-MB 231(MT1-MMP-positive) bearing mice and weak uptake for A549 (MT1-MMP-negative) tumor bearing model	[108]
FROP-1 (EDYELMDLLAYL)	Radiolabeling with iodination using the chloramine-T with specific activities 90 GBq/mmol for the ^{125}I-labeled peptide and 110 GBq/mmol for the ^{131}I-labeled peptide after purification	i After 5 min incubation of radiopeptide with human serum, degradation was started and after 120 min of incubation time, the full-length peptide was completely degraded ii Highest and specific binding capacity to FRO82-2 and MCF-7 cancer cells iii Fast internalization to MCF-7 cells started after 10 min and reach to maximum after 60 min incubation iv IC_{50} for FRO82-2 cells was approximately 8 mM, and that for MCF-7 cells was about 12 mM v Main exertion way from liver and kidneys vi Maximum specific tumor uptake for both FRO82-2 and MCF-7 cancer cells after 15 min and maximum tumor/muscle ratio after 135 min	[109]
FROP-DOTA	Radiolabeling with ^{111}In chloride at the C-terminal end of the peptide via an additional lysine with 95% radiochemical purity after purification	i After 15 min incubation of radiopeptide with human serum, degradation was started and after 120 min of incubation time (half-life of 71 min) ii For FRO82-2 cells accumulation up to 40% of the applied dose after 4h and for MCF-7 up to 90% of the applied dose after 2h iii Maximum specific tumor uptake for SW1736 and HNO-223 cancer cell after 3h incubation without significant binding to the non-tumor cell line HPV-16-GM and the primary endothelial cells (HUVEC) iv IC_{50} = 494 nM for FRO82-2 cells v Main exertion way from liver and kidneys vi Maximum specific tumor uptake for FRO82-2 after 5 min equal to 1.6 and for MCF-7 cancer cells after 15min Vii Maximum tumor/muscle ratio equal to 2.7 after 5 min p.i	[110]
FROP-DOTA-PEG	Attachment of FROPDOTA to CH3O-PEG(20 000)C2H4-maleimide and radiolabeling	i Slow binding kinetics than FROPDOTA	[111]

(*continued on next page*)

Table 1 (*continued*)

Peptide name and sequence	BFCA and radionuclide	Results	Ref.
	with ^{111}In chloride at the C-terminal with 95% radiochemical purity after purification	ii Maximum specific tumor uptake for FRO82-2 after 120 min p.i equal to 2.3 iii Maximum tumor/muscle ratio equal to 4.1 after 24h p.i	
HYNIC-(Tricine/EDDA)-FROP	Radiolabeling with ^{99m}Tc radionuclide at the C-terminal end of the peptide via Tricine/EDDA as coligand with 99.6% radiochemical purity without further purification	i *In vitro* stability 99% up to 6 h in normal saline ii *In vitro* stability 98% up to 1h incubation at 37 °C in human serum iii Maximum specific tumor uptake for MCF-7 cancer cells after 1h incubation and low binding to non-tumor HFFF-2 cell line iv 10.6% internalization to MCF-7 cells after 30 min and 18.3% after 6 h incubation v K_D and B_{max} equal to 158 nM and 4.5 ± 0.6 × 10^7 site per cell respectively vi rapidly cleared from the blood circulation due to the mainly renal exertion vii maximum specific tumor uptake (0.38% ID/gr) and tumor/muscle: 3 to MCF-7 cells after 15 min viii Good ability for MCF-7 tumor visualization at 15min with high tumor-to-background contrast	[55]
HYNIC-(Tricine)-FROP	Radiolabeling with ^{99m}Tc radionuclide at the C-terminal end of the peptide via Tricine as coligand with 99.5 % radiochemical purity without further purification	i *In vitro* stability 97% up to 6 h in normal saline ii *In vitro* stability 97% up to 1h incubation at 37 °C in human serum iii Maximum specific tumor uptake for MCF-7 cancer cells after 1h incubation which was blocked (6.7 fold) with excess of FROP-1 iv 4.8% internalization to MCF-7 cells after 30 min and 7.4% after 4 h incubation v K_D and B_{max} equal to 154 nM and 7.4 ± 0.7 × 10^6 site per cell respectively vi Rapidly cleared from the blood circulation due to the mainly renal exertion vii Maximum specific tumor uptake (5.1% ID/gr) and tumor/muscle: 3.8 to MCF-7 cells after 15 min	[54]
^{111}In-A20FMDV2	Radiolabeling with ^{111}In	i *In vitro* stability 97% up to 24 h in PBS ii *In vitro* stability 50% up to 4h incubation at 37 °C in mouse serum iii IC_{50} = 1.73 ± 0.46 nM for A375Pβ6 cell line iv (89–96)% internalization to A375Pβ6 cells after 60 min v Tumor-to-Muscle (7) and Tumor-to-Blood (9) at 1 h post-injection for A375Pβ6 cell line vi Good ability for MCF10A.DCIS.COM and MCF10A.CA1a breast carcinoma cell lines at 60 min with high tumor-to-background contrast	[112]
^{99m}Tc-(CK3)	Radiolabeling with ^{99m}Tc	i High capacity binding to MDA-MB-231 breast cancer cells ii Maximum tumor uptake after 4 h p.i iii Good ability for visualization of MDA-MB-231 breast tumor with high contrast at 4 h	[113]
^{111}In-A9	Radiolabeling with ^{111}In with high radiochemical purity up to 95%	i Good *in vivo* stability ii High affinity in the range of nanomolar (4.9 nM and 103 nM) iii Putative internalization to metastases BT474 breast cancer cells iv Fast clearance from blood circulation v Low radioactivity accumulation in the gastrointestinal	[114]
(^{131}I-^{125}I)-p160	Radiolabeling with iodide	i High capacity binding to MDA-MB-435 and MCF-7 breast cancer cells ii Rapid internalization in MDA-MB-435 and MCF-7 breast cancer cells iii $IC_{50,}$ Kd and B_{max} equal to 0.6 μmol/L, 0.8 μmol/L and 1.03 ± 0.6 × 10^{11} sites per cell respectively iv Fast tumor uptake 1h in MDA-MB-435 breast cancer tumor with low non-target accumulation	[115–117]

1.4. ^{99m} Tc-αM$_2$ and ^{99m}Tc-MAG3-αM$_2$ peptide

A pentadecapeptide (αM$_2$) was synthesized based on overcome some of the difficulties associated with monoclonal antibodies, while preserving affinity. A peptide that is the smallest possible molecule derived from the original antibody was developed based on the CDR and framework regions of the idiotype of a murine antitumor monoclonal antibody (ASM2), which has specificity against the pan-carcinoma cell-surface antigen, polymorphic epithelial mucin, detected by the parent antibody [100]. The amino acid sequence of (αM2) peptide was YCAREPPTRTFAYWG that the presence of cysteine and tyrosine residues allows for radiolabeling with technetium-99 m via direct method [101]. The immunological affinity of this peptide for specific binding site is mainly based on the Glu-Pro-Pro-Thr (EPPT) residues in its sequence. In comparison to parent antibody, the affinity of the (αM2) peptide was significantly lower (approximately 20 fold less). *In vivo* evaluation of this radiolabeled peptide was studied in women with breast cancer. The radiolabeled peptide showed favorable kinetics and

despite rapid excretion from kidneys, the peptide was localized in tumor organ (images were obtainable as early as 30 min after injection). The mean tumor/non-tumor ratio for ^{99m}Tc-(αM2) peptide was reported between 2 from 4 in patients. ^{99m}Tc-(αM2) peptide has good ability for primary and metastatic tumor sites such as axillary and supraclavicular lymph nodes in patients after 3 h p.i. Although αM2 peptide is derived from an antibody structure, but can preserve the affinity for its receptor. With respect to this fact that for an ideal molecular imaging agent, fast, accurate, and clear tumor visualization are required [64,65], two main quotations are existed for ^{99m}Tc-(αM2) peptide can recognize neoplastic lesions *in vivo* in patients with primary and metastatic breast carcinoma. One of them is the high background cardiac blood pool at early time points that limited the application of radiolabeled peptide for visualization of other organ metastasis such as lungs, mediastinum, chest wall, and liver. The other quotation is false-positive uptake in normal nipple and areola area in 71% of patients. ^{99m}Tc-(αM2) peptide didn't have any adverse reaction during the study or follow-up of up to 9 months.

In another study, Okarvi prepared ^{99m}Tc-(αM2) via direct labeling method and $(MAG)_3$-derivatized αM_2 peptide with replacing cysteine residue, in the position 2 by alanine and triproline $(Pro)_3$ residue as a spacer for comparing the *in vitro* and *in vivo* characteristics of these radiolabeled peptides [102]. ^{99m}Tc-MAG3-αM_2 showed good *in vitro* and *in vivo* stabilities which were confirmed by transchelation study in the presence of excess cysteine. ^{99m}Tc-aM2 has comparable but lower *in vitro* stability than ^{99m}Tc-MAG_3-αM_2 that attributed to the relatively weaker bond strength cause by the weaker complex formation via cysteine moiety. *In vitro* cell accumulation of ^{99m}Tc-MAG3-aM2 and ^{99m}Tc-aM2 in human breast cancer cells (MCF-7 and MDA-MB-231) approximately has a similar profile for all time point between from 15 to 120 min; however, ^{99m}Tc-MAG_3-αM_2 showed a relatively higher cellular uptake than ^{99m}Tc-aM_2. Maximum internalization of ^{99m}Tc-MAG_3-αM_2 into MCF-7 cells occurred after 60 min incubation. Biodistribution of ^{99m}Tc-αM_2 and ^{99m}Tc-MAG_3-αM_2 in normal mice demonstrated that ^{99m}Tc-MAG_3-αM_2 had a faster blood clearance and superior urinary excretion properties than ^{99m}Tc-αM2. Biodistribution of these radiolabeled peptides at 60 min p.i. in nude mice bearing MDA-MB-231 xenograft showed approximately similar tumor uptake, although ^{99m}Tc-MAG_3-αM_2 exhibited a considerably lower uptake (Tumor/Blood = 1.2) and retention by the kidneys than ^{99m}Tc-αM2 (Tumor/Blood = 1.9). The main different organ uptake between ^{99m}Tc-αM2 and ^{99m}Tc-MAG3-aM2 was found for intestine (4.3% ID/gr for ^{99m}Tc-αM2 v.s 14.4 %ID/gr for ^{99m}Tc-MAG3-aM2 (Table 1).

Structure modification of αM2 peptide for improving the unfavorable pharmacokinetic and imaging properties of ^{99m}Tc-αM2 with retaining most or all of the original affinity and specificity lead to development of ^{99m}Tc-MAG_3-αM_2. On the other hand, a major drawback of the direct labeling such as lack of control over chelate-metal non-specific binding that lead to poor stability of complex was the main reason for indirect labeling method for αM2 peptide [103]. The using of chelator and spacer is one of the facile strategies for preparation and pharmacokinetic modifications (receptor-binding and biological characteristics) of peptide-based radiopharmaceuticals for *in vivo* application [104]. Good ability for formation of stable complex with ^{99m}Tc and $^{186/188}$Re radionuclides for possible *in vivo* diagnostic and therapeutic applications and particularly increasing the degree of urinary excretion were the main reasons for choosing the MAG3 as a chelator for radiolabeling of αM2 peptide [105,106]. In comparison to ^{99m}Tc-αM2 the main superiority of ^{99m}Tc-MAG_3-αM2 was the rapid clearance from the blood circulation, however fast clearance from blood circulation obstacles the efficient accumulation of ^{99mTc}-MAG_3-αM_2 in tumor tissue. With consideration of low tumor uptake for several radiolabeled peptides, such as ^{99m}Tc-labeled bombesin analog (^{99m}Tc-RP527) [107,108], this radiolabeled peptide when tested in human, provided good imaging of tumor. Therefore, ^{99m}Tc-MAG_3-αM_2 could have been potential for clinical tumor imaging. It is necessary to mention that the high gastrointestinal uptake for both ^{99m}Tc-αM2 and ^{99m}Tc-MAG_3-αM_2 is the main limitation for the imaging of tumors and their metastases in the abdominal area. Therefore, the appropriate modification in the structure of original αM_2 peptide or using hydrophilic amino acid (i.e. aspartic acid or ɣ-aminobutyric acid) is required for improving the pharmacokinetic characteristics of this radiolabeled peptide.

1.5. Patched receptor targeting ^{99m}Tc-radiolabeled peptides for hedgehog positive breast tumors

The hedgehog (Hh) signaling pathway plays a critical role in promoting malignant cell growth including pancreatic, gastric, lung and breast cancers in a ligand dependent manner [109–115]. The Hh signaling pathway has three kinds of ligands, Sonic Hh (Shh), Desert Hh (Dhh), and Indian Hh (Ihh) that in the absence of ligand stimulation, the activation of the Hh signaling pathway was suppressed. The activation of Hh signaling which the transmembrane protein Patched-1 (Ptch1) mediated is related to tumor cell growth, metastases and invasion. Cyclopamine as an alkaloid that has been acted as an inhibitor for the Hh signaling pathway to suppress tumor cell growth *in vitro* and *in vivo*. However, no drug has been developed to control the Hh signaling at the clinical practice. Radioiodinated PTCH-1 ligand sonic (^{131}I-SHH) had a significant accumulation in tumor tissue as compared to normal organs (tumor to-muscle ratio was approximately 8:1 at 5 h) that express the ability of this radiolabeled protein for *in vivo* detection of breast tumor with high Hh signaling [116]. Previously Nakamura research group demonstrated that anti-Ptch1 polyclonal antibodies which recognize an oligopeptide of Ptch1 on the Hh positive cancer cell surface that might be useful as a promising tool for targeting cancer-cell surface for the cancer diagnosis and therapy [117]. The sequence of this target was the short amino acid sequence of Ptch1 (KADYPNIQH), which was located in the putative docking site of the Hh ligand, and Ptch1 [118,119]. This program employed a genetic algorithm [120,121], therefore Nakamura et al. designed seven peptide sequences using this program.

Sims-Mourtada et al. demonstrated strong detection of tumor xenografts using an iodinated derivative of the PTCH-1, but its clinical utility was limited due to poor stability and pharmacokinetics [116]. For this problem solving, this research group developed radiolabeled peptides which dock inside the PTCH receptor. Among several peptides which were previously reported by Nakamura et al. two peptide sequences (FAPVLDGAVSTLLGV or peptide A) and (DNTRYSPPPPYSSHS or peptide B) were selected for targeting the PTCH receptor on breast cancer cells and breast cancer stem cell-enriched populations [119,122]. Fluorescence microscopy of breast cancer cell lines revealed significant uptake of the FITC-tagged peptides in a panel of breast cancer cell lines (MCF-7 > SUM159 > 13762 > SkBr3 > T47D > IBC3 cells uptakes). Fluorescence microscopy using anti-PTCH antibodies on cells treated with FITC-labeled PTCH-binding peptides revealed that this binding was specific to the PTCH receptor. For ^{99m}Tc-labeling, N, N′-ethylene-di-*L*-cysteine (EC) chelator was selected and lysine residue was used as a linker [122]. *In vitro* cellular uptake of the ^{99m}Tc-conjugated peptide in three breast cancer cell lines, SUM159, MDA-IBC3, and 13762 showed significant cellular uptake in all cell lines. The SUM159 cell line showed the highest radiotracer uptake; however significant uptake of the radiotracer was also observed in two other cell lines (increasing steadily in MDA-IBC3 and reaching saturation in 13762 cell lines). The utility of ^{99m}Tc-EC-peptide A for imaging of the PTCH receptor in breast cancer was demonstrated with planar scintigraphy in mice bearing 13762 breast carcinoma xenografts. Planar scintigraphy at 1, 2, and 4 h after injection of the radiolabeled peptide showed good tumor uptake up to 4 h p.i. Also an average tumor-to-muscle ratio of 4.5 was obtained at 1 h and 5.4 at 4 h that may serve as useful theranostics which may be used to both imaging and treatment of breast cancer. High liver uptake for ^{99m}Tc-EC-peptide-A attributed to the both clearance of the peptide from liver and low-level endogenous

expression of the PTCH receptor by liver tissue.

In various studies reported that Hh signaling has important role in breast cancer progression and metastasis. Sonic hedgehog (Shh) are overexpressed in invasive ductal carcinoma that has low prognosis. Peptide A successfully radiolabeled with ^{99m}Tc radionuclide with using EC chelator that has good stability and efficient binding for conformation oxotechnetium complex. ^{99m}Tc-EC-peptide A was used for targeting of PTCH receptor on breast cancer cells and breast cancer stem cell. This radiolabeled peptide had specific binding to cancer cell lines that overexpressed PTCH receptor and binding intensity directly corresponded to PTCH expression. Good tumor uptake and tumor/muscle ratio after 4 h p.i, demonstrated the ability of this radiolabeled peptide for targeting and imaging of PTCH overexpressed tumors [122]. With respect to this fact that hedgehog signaling induces resistance to chemotherapy upregulation of PTCH receptors could have been occurred after chemotherapy [123–125]. Therefore, ^{99m}Tc-EC-peptide A may offer as a useful radiotracer to assess resistant tumor tissue after chemotherapy treatment and noninvasively follow response to chemotherapy due to the high expression of hedgehog receptors by residual cells. It is reported that hedgehog signaling is required for the growth of breast cancer stem cells and followed with high expression levels of the PTCH receptors [126]. Therefore, ^{99m}Tc-EC-peptide A may serve as a ligand to detect and target of malignant mammary stem cells.

1.6. ^{99m}Tc-TP1623 peptide for HER2 positive breast cancer

Alan Berezov et al. found that YCFPDEEGACY peptide sequence, as a small molecular mimic peptide of HER2, had a high specific affinity for HER2 [127]. The peptide sequence YCFPDEEGACY was coupled to bifunctional chelator as MAG3 in amino terminal [128–130]. ^{99m}Tc-TP1623 peptide showed good *in vitro* stability at room temperature (up to 93% after 6 h) and serum stability up to 86% after 24 h incubation with human serum. Cell binding activity of ^{99m}Tc-TP1623 was evaluated on SKBR-3 (HER2 positive) and MDA-MB-231 (HER2 negative) breast cancer cells. The *in vitro* receptor binding experiment demonstrated that the binding of ^{99m}Tc-TP1623 to SKBR-3 cells was concentration dependence. This binding was specific and competitively inhibited in the presence of excess TP1623 peptide. The internalization percentage of ^{99m}Tc-TP1623 (18% after 8 h incubation) into SKBR-3 cells due to the binding with HER2 receptors on the cells surface was low. Biodistribution of ^{99m}TC-TP1623 showed fast urinary excretion in normal mice resulted in reduction of radioactivity in blood circulation after 120 min p.i. Low activity in thyroid and gastric demonstrated high *in vivo* stability for ^{99m}TC-TP1623. SPECT/CT imaging results of ^{99m}TC-TP1623 in SKBR3 human breast cancer nude mice showed good tumor visualization at 30 min (tumor/non-tumor ratio was 2.19) after injection and reached the peak at 120 min (tumor/non-tumor ratio was 5.18). However, the tumor was still visible at 4 h (tumor/non-tumor ratio was 3.49). Tumor accumulation of ^{99m}TC-TP1623 in mice that were treated with non-labeled TP1623 significantly was reduced about 80%, that demonstrated the specific HER2 binding for this radiotracer.

Due to the importance of HER2 overexpression in breast cancer, that mostly has poor prognosis and fast invasive, a small radiolabeled peptide ^{99m}TC-TP1623 for feasible targeting and imaging of HER2-positive breast cancer cells was developed. Radiolabeling of TP1623 peptide without any further isolation and purification was easily prepared by one-step freeze-dried kit. The binding of ^{99m}TC-TP1623 to HER2 positive SKBR-3 cancer cell line was specific and concentration dependent and significantly blocked in the presence of excess of TP1623 peptide. This binding mainly mediated by HER2 cell surface receptor that was confirmed by the *in vitro* and *in vivo* blocking studies. Although, low internalization and high radioactivity in cell surface demonstrated the avid binding to the HER2 receptor. *In vivo* biodistribution of ^{99m}TC-TP1623 demonstrated fast clearance from blood circulation and low blood pool radioactivity in non-tumor organs especially in lungs and heart. Tumor accumulation was mainly mediated by HER2 receptor and confirmed by low accumulation in MDA-MB-231 HER2 negative cancer cell line and reducing the tumor/non-tumor ratio by a factor of 5 after the injection of excess TP1623 peptide. Fast tumor uptake at early time (30 min) after p.i led to the short time interval of image acquisition. These characterizations offer the ^{99m}TC-TP1623 radiolabeled peptide as a suitable tumor-imaging probe for tumors with high overexpression of HER2 receptor. ^{99m}TC-TP1623 showed low tumor uptake in brain, suggesting that the radiolabeled peptide unable to penetrate into blood–brain barrier and could be used to assess the integrity of the blood–brain barrier. The main manifest ability of ^{99m}TC-TP1623 is low intestine accumulation that assembles the imaging of HER2 positive tumors in the abdominal area. However, long-term activity retention in the kidneys and bladder result in limited visualization of nearby tumors. Therefore, pharmacokinetic modification for increasing the speed clearance from kidneys and maybe *in vivo* stability be necessary.

1.7. ^{111}In-DOTA-(GSG)-KCCYSL for HER2 receptor-expressing breast carcinoma

Six-amino-acid KCCYSL peptide, as a HER2-avid peptide, discovered from bacteriophage display after *in vitro* selection with a recombinant HER2 extracellular domain by Karasseva research group [131]. Sequence analysis suggested that the KCCYSL peptide acts as a mimetic of a CCY/F motif presents in the epidermal growth factor–like domain of HER2 ligands and specifically recognized recombinant HER2-ECD and human carcinoma cells overexpressing HER2 receptor. Therefore, this research group hypothesized that the KCCYSL peptide has potentially been used as an imaging agent for HER2 overexpressing tumors for diagnostic purposes. Due to the specificity, affinity (351 ± 32 nM), and key binding residues of KCCYSL peptide to HER2 receptor, in another study the optimized peptide sequence (^{111}In-DOTA-(Gly-Ser-Gly)-KCCYSL) was developed by Kumar et al. [132] for tumor targeting. To this aim, DOTA as a bifunctional chelator was coupled to the NH_2 terminus of the KCCYSL or KYLCSC (scrambled) peptide with a (GSG) amino acid spacer between DOTA and the NH_2-terminal lysine of the peptide to avoid any steric hindrance by DOTA. ^{111}In-DOTA-(Gly-Ser-Gly)-KCCYSL was radiochemically stable in phosphate buffer saline up to 12 h. According to the metabolic stability of the radiolabeled peptide, it was intact at least up to 60 min. *In vitro* cell binding experiments showed that the receptor-binding activity of the radiolabeled peptide to MDA-MB-435 (HER2 positive) human breast carcinoma cells increased gradually at time-depended incubation and reached its maximum uptake at 2 h. Minimal binding was observed to K-562 human chronic myeloid leukemia cells (HER2 negative), indicating that the radiolabeled peptide was specific for HER2 expressing human breast cancer cells. This specific binding for ^{111}In-DOTA-(GSG)-KCCYSL peptide was confirmed by competition experiments as a decreased binding in the presence of various concentrations of non-radiolabeled peptide. The IC_{50} value of ^{111}In-DOTA-(GSG)-KCCYSL for MDA-MBA-435 breast carcinoma cells was found 42.5 ± 2.76 nM, while the affinity of KCCYSL for its target was approximately 300 nM. Internalization results indicated that the cell-surface associated radioactivity increased until 2 h and the progressive accumulation of total radioactivity inside MDAMB-435 carcinoma cells was occurred via receptor-mediated endocytosis as 11%. The most peptide binding occurred on the cell surface. A reduced tumor uptake profile was observed at various times (15 min-24 h) after injection of ^{111}In-DOTA-(GSG)-KCCYSL in MDA-MB-435 breast tumor–bearing mice. In comparison to this tumor uptake profile, the reducing of blood activity occurred very fast. This fast blood clearance of this radiolabeled peptide resulted in a tumor-to-blood ratio of 5.0 at the end of 2 h, that was 7.4 times higher than the ratio (0.67) obtained 15 min p.i. The maximum normal organ uptake was seen in the kidneys due to the primary route of excretion. A whole-body SPECT/CT imaging in SCID mice bearing HER2 positive MDAMB-435 breast tumors confirmed that ^{111}In-DOTA-(GSG)-KCCYSL has good ability for tumor visualization at 2 h p.i, which was coincident with a

reasonable tumor-to-blood ratio.

At early time point after injection, ^{111}In-DOTA-(GSG)-KCCYSL showed fast tumor uptake; unfortunately, tumor uptake was not consisted and rapidly decreased. One main reason to this fact could have been attributed to the lysosomal degradation within renal cells and degradation with peptidase which was started after 1 h p.i. One of the other main quotation is that the lungs displayed appreciable retention of radioactivity attributed to the contribution of the blood pool and free disulfide bond moiety that is the main obstacle for breast imaging [132]. ^{111}In-DOTA(GSG)-KCCYSL shows promise for clinically imaging tumors based on tumor-associated HER2 expression.

1.8. ^{111}In-DOTA-1-D03 peptide

Tumor vasculature proteins including vascular endothelial growth factor, $\alpha_v\beta_3$ integrin, and platelet derived growth factor serve as potential targeting agents for cancer imaging and therapy [133,134]. The EGFL6 is an approximately 60 kDa secreted protein with epidermal growth factor (EGF) structural homology that is expressed in various tumors [135,136]. As mention above, the enhancing of specific tumor accumulation, imaging ability and rapid clearance form blood circulation are primary goals for KCCYSL peptide as a HER2 targeting peptide. A phage microlibrary was engineered by *in vivo* phage display affinity maturation; and second generation 1-D03 (MEGPSKCCYSLALSH) and 3-G03 (SGTKSKCCYSLRRSS) peptides were selected [137]. 1-D03 peptide showed higher specificity for MDA-MB-435 cells than 3-G03 because 1-D03 bound only MDA-MB-435 cells, while 3-G03 appeared to bind all of the carcinoma cell lines (human prostate (PC-3), pancreatic (Panc-1), and breast (BT-549) tested, however this binding had low affinity to these cell lines. The results of *in vitro* binding assay showed that 1-D03 and 3-G03 bound to HER2 with affinities of 236 ± 83 nM and 289 ± 13 nM, respectively, and both affinities significantly were higher than the parent peptide KCCYSL (351 ± 32 nM). According to fluorescent imaging results, this binding was not seen for 184A.1 normal breast endothelial cells. To further assess of binding (DOTA-1-D03) and (DOTA-3-G03) peptides were chemically synthesized and radiolabeled with ^{111}In. The stabilities of both peptides in buffer and mouse serum were observed up to 24 h. *In vitro* cell binding results confirmed retained specificity (ratio of MDA-MB-435 to 184A.1 binding) and affinity for both DOTA-conjugated peptides. ^{111}In-DOTA-1-D03 showed higher binding (1,681 ± 119 CPM) and specificity (specificity ratio of 7.44) to MDA-MB-435 than KCCYSL (1,038 ± 106 CPM and specificity ratio of 3.49. However, binding and specificity of ^{111}In-DOTA-3-G03 were found 1,494 ± 141 CPM and 1.4 respectively. The high specific and binding of the ^{111}In-DOTA-conjugated 1-D03 peptide to MDA-MB-435 cells provided the necessary evidence to continue into animal studies, that was performed in mice-bearing MDA-MB-435 human breast tumor xenografts. The maximum tumor to blood and tumor to muscle ratios were 6.02 and 17.9 after 2 h p.i, respectively, while these ratios were 5.08 and 22 for KCCYSL peptide. The nonspecific bindings of ^{111}In-DOTA-1-D03 in comparison to KCCYSL peptide were low in heart (0.130 ± 0.03 %ID/g versus 0.22 ± 0.04 % ID/g), lung (0.40 ± 0.04 %ID/g versus 0.82 ± 0.14 %ID/g), muscle (0.04 ± 0.01 %ID/g versus 0.09 ± 0.02 %ID/g), and bone (0.09 ± 0.04 %ID/g versus 0.20 ± 0.03 %ID/g). In comparison to KCCYSL peptide, ^{111}In-DOTA-1-D03 showed fast blood exertion and low blood maintain (0.06 ± 0.01 %ID/g versus 0.13 ± 0.03 %ID/g). Also total kidney retention for the 1-D03 was significantly less than KCCYSL kidney uptake at 2 h p.i (4.746 ± 0.3 %ID/g versus 5.75 ± 0.6 %ID/g). Whole body SPECT/CT at 2 h p.i of ^{111}In-DOTA-1-D03 peptide demonstrated clear tumor uptake and tumor visualization of the radiotracer in MDA-MB-435 tumor-bearing SCID mouse. This tumor uptake was specific and significantly eliminated with pre-injection of non-labeled peptide at 15 min before injection of radiotracer [137].

To sum up, creation of an improved HER2-targeted radiolabeled imaging peptide based on a KCCYSL core sequence has some prosperity and deflection. In comparison to antibody, KCCYSL peptide has superior ability for specific targeting of HER2 expression tumors. This binding mainly mediated by receptor as, it does not bind cancer cells devoid of the HER2 receptor. In other to optimization of KCCYSL peptide for improving pharmacokinetic properties for reaching to the highest tumor uptake with minimal non-target uptake and similar affinity as the parent peptide, spacer or chelate modification lead to development of ^{111}In-DOTA-1-D03. ^{111}In-DOTA-1-D03 showed better *in vitro* characterizations such as high affinity and specificity than radiolabeled KCCYSL to MDA-MB-435 cells. Radiolabeled peptide ^{111}In-DOTA-1-D03 showed fast tumor uptake at early time point after injection and reached to the maximum tumor uptake after 30 min p.i. With the passing time, the accumulated activity in tumor tissue was reduced, as this reduction from blood circulation was faster than KCCYSL peptide and lead to the maximum T/M and T/B ratios after 2 h. In comparison to KCCYSL, ^{11}In-DOTA-1-D03 peptide had an equal tumor to blood ratio at 1 h and a significantly higher tumor to blood ratio at 2 h p.i. ^{111}In-DOTA-1-D03 had low accumulated activity in heart however, for lung tissue the accumulated activity (especially after the starting of the injection) was more than tumor tissue and after 2 h p.i, lung uptake was slightly lower than the tumor uptake. These non-target accumulations in heart and lungs may not assemble the imaging of HER2 positive tumors in the breast tissue. ^{111}In-DOTA-1-D03 had good ability for HER2 positive MDA-MB-435 breast tumor visualization, which mainly was disappeared in the presence of non-labeled peptide competitor. Inability in the reducing of kidneys uptake with pre-injection of non-labeled peptide before imaging strongly demonstrates that the kidneys retention is sequence independent and could have been the other reasons. Therefore, *in vivo* phage display affinity maturation of HER2-targeting peptide indeed to improve KCCYSL pharmacokinetics such as enhancing tumor specificity and reduction non-target retention and may serve as a useful clinical probe for HER2-expressing malignancies but future investigations are needed for reducing non-target radioactivity.

1.9. ^{111}In-DOTA-51 peptide as SPECT imaging for resistance-susceptible breast cancer

Due to the importance of early diagnosis of breast cancer specially in the case of resistant BT-474 human breast cancer cells to both tamoxifen and trastuzumab, *in vivo* phage display was used to selection of peptide 51(ATWLPVPVVGYFMASA) by Benjamin et al. [138] as a peptide for SPECT imaging of BT-474 human breast cancer. According to the fluorescent microscopy assay, the peptide bound to BT-474 human breast cancer cells and had no detectable binding to 184A.1 normal breast epithelial cells. Flow cytometry results demonstrated that peptide 51 bound with moderate affinity for BT-474 cells with EC_{50} 2.33 ± 0.66 μM. However, this binding was minimal for normal breast tissue. For more *in vitro* and *in vivo* evolution, full-length 51 peptide was conjugated to DOTA at N-terminal with GSG spacer and radiolabeled with ^{111}In. *In vitro* cell binding revealed that the peptide affinity had not been diminished by addition of a DOTA chelator and radiolabeling and the affinity was retained (16 ± 7 nM). For *in vivo* evaluation, ^{111}In-DOTA-51 was injected into mice bearing BT-474 human breast cancer xenografts. At 2 h post-injection tumor uptake was found 0.12 ± 0.02 %ID/g and tumor to blood ratio and tumor to muscle ratio were determined to be 2.3 and 7.1 respectively. The tumor uptake was specific and uptake organs that could produce background signal for breast cancer imaging, including the heart (0.04 ± 0.01 %ID/g), and lung (0.13 ± 0.03 %ID/g) were low indicating tumor uptake was not mediated by blood pooling. For this radiolabeled peptide, kidney uptake was found 30.4% ID/g that attributed to the excretion way from kidneys. It is necessary to mention that ^{111}In-DOTA-51 had low tumor uptake under 1 %ID/g. Therefore, due to the low non-target uptake especially in heart and lung, ^{111}In-DOTA-51 has reasonable tumor to

blood and tumor to muscle ratios as similar and comparable with vasculature targeting RGD peptide. In comparison to Nrp-1 targeted V1 peptide (ATWLPPR), V1 peptide had high tumor uptake (2% ID/g for V1 peptide), but its tumor to muscle ratio was significantly low (0.22) [139]. SPECT/CT imaging of ^{111}In-DOTA-51 peptide revealed high tumor uptake, as tumor at 2 h post-injection was well detectable.

However, the application of ^{111}In-DOTA-51 in clinic as imaging agent may restricted with two main reasons. One of this reason attributed to the high non-target lung tissue radioactivity (equal and even higher than tumor uptake) after 2 h p.i that may obstacle the imaging of breast tumor and metastasis. The other reason attributed to the abdominal radioactivity accumulation especially in intestines that not offer good ability for imaging of HER2 positive tumor in this area. Therefor imaging ability of ^{111}In-DOTA-51 is limited for only BT-474 breast cancer cells. Briefly, ^{111}In-DOTA-51 radiolabeled peptide may have a potential application for imaging of BT-474 human breast tumor and other HER2 positive tumors if the suitable pharmacokinetic modification for reducing the non-target accumulation was carry out.

1.10. ^{111}In-DOTA-(GSG)-G3-C12 peptide for targeting Galectin-3 overexpressing tumor

Galectin-3, a 30-kDa protein, is associated with tumor growth and metastases in several types of cancer, particularly in breast cancer [140–144]. Given this fact, Galectin-3 can be used as a useful protein for noninvasive imaging of tumors expressing this protein. The interaction of galectin-3 with various ligands dictates its cellular localization and facilitate metastasis by promoting tumor cell adhesion and invasion, inhibiting tumor cell apoptosis, and inducing endothelial proliferation and angiogenesis [145–150]. It is necessary to mention that peptide-based antagonists bind to a unique region of galectin-3 and may offer greater specificity than the carbohydrate based inhibitors. G3-C12 peptide (ANTPCGPYTHDCPVKR), as a peptide-based antagonists of galectin-3, was obtained from bacteriophage display selections. This peptide has remarkable specific binding to galectin-3 but not to other galectin family members. G3-C12 peptide binds to the C-terminus CRD region of galectin-3 and has the ability of reorganization cell surface galectin-3, that is expressed on breast carcinoma cells. Zou et al. [151] hypothesized that this peptide may form the basis for an imaging agent to monitor breast carcinoma cells growth and metastasis *in vivo* [152,153]. Therefore, they used a radiolabeled tracer of the G3-C12 peptide as a SPECT/CT agent for galectin-3 expressing human breast tumors. To this aim, NH_2 terminus of linear G3-C12 peptide was conjugated to DOTA via a Gly-Ser-Gly (GSG)–linker between radionuclide and peptide sequence and then was radiolabeled with ^{111}In [154]. ^{111}In-DOTA-(GSG)-G3-C12 was stable for 12 h in phosphate buffer saline and as well as in serum (85%) and urine (80%) at 30 min after injection of radiolabeled peptide in mouse. *In vitro* binding affinity of ^{111}In-DOTA-(GSG)-G3-C12 for galectin-3, showed significant binding to human MDA-MB-435 (galectin-3 positive) and negligible binding to BT549 (galectin-3 negative) breast carcinoma cells, indicating that the radiolabeled peptide was specific for galectin-3 expressing human breast cancer cells. This binding was occurred on the cell surface, and no internalization of the peptide was observed. Competition experiments in the presence of the increased concentrations of non-radioactive ^{111}In-DOTA-(GSG)-G3-C12 peptide, showed the decreased binding of the radiolabeled peptide to the MDA-MBA-435 breast carcinoma cells (IC_{50} value was found 200 nM). This binding affinity is comparable to the affinity of G3-C12 of 88 ± 23 nM for recombinant galectin-3. The biodistribution of the ^{111}In-DOTA-(GSG)-G3-C12 peptide in mice bearing MDAMB-435 human breast tumors showed the rapid and specific tumor uptake and blood clearance kinetics resulted in a tumor-to-blood ratio of 8.6 at the end of 2 h, a value 12 times higher than the ratio (0.70) obtained after 30 min post injection (Table 1). The whole body SPECT/CT scan in mice bearing galectin-3 expressing MDA-MB-435 human breast tumors at 2 h after injection showed that breast tumor was clearly visualized with high tumor-to-background contrast. Overhead due to the good pharmacokinetics characterizations, ^{111}In-DOTA-(GSG)-G3-C12 peptide has potential as a radiopharmaceutical for imaging of galectin-3 expressing breast tumor in clinical practice [154].

1.11. ^{99m}Tc-(HYNIC-AF7p)(tricine)(TPPTS) peptide-based probe targeting MT1-MMP

Matrix metalloproteinases (MMPs), are a family of zinc-dependent endopeptidases, play an important role in the development of cancer that not only have distinct roles in tumor angiogenesis, but also affect multiple signaling pathways to control the balance between growth and antigrowth signals in the tumor microenvironment [155–157]. MMPs overexpress in patients with breast cancer and the potential of utilization MMP as target for breast cancer diagnosis was reported in some studies [158–160]. The specific MT1-MMP targeting peptide would provide the ability of earlier detection of breast cancer that overexpressed MT1-MMP. Zhu et al. [160] developed a high MT1-MMP affinity peptide, named AF7p, by phage display peptide library screening technique. According to this study, near infrared dye labeled AF7p demonstrate the potential of utilizing AF7p for MT1-MMP targeted tumor detection. Due to the more sensitivity and accuracy of radioisotope mediated imaging technique, Kaiyin et al. modified AF7p peptide with HYNIC chelator and developed it for MDA-MB-231 (MT1-MMP positive) breast cancer detection [161]. HYNIC-AF7p was synthesized and radiolabeled with ^{99m}Tc to form the ternary ligand complex [^{99m}Tc](HYNIC-AF7P)(tricine)(TPPTS). [^{99m}Tc]-(HYNIC-AF7P)(tricine) (TPPTS) showed good *in vitro* stability after 6 h incubation with normal saline and excess amount of cysteine up to 96%. According to the fluorescent immunohistochemistry results, strong fluorescent signals were seen for MDA-MB-231 cells treated with Cy5.5-AF7p, while little signals were found in A549 (Low expression of MT1-MMP) cells. This binding was specific and blocked in the presence excess amount of non-labeled AF7p. Biodistribution of [^{99m}Tc](HYNIC-AF7P)(tricine) (TPPTS) in BALB/c nude mice bearing MDA-MB-231 human breast cancer xenografts showed maximum tumor uptake after 0.5 h p.i. The maximum T/M = 4.17 and T/B = 11.11 ratios were obtained at 2 h p.i. In comparison to tumor uptake, the accumulated activity in non-target organs especially in lungs, heart and intestines were low that offer the imaging of tumor in breast tissue and abdominal area. The kidneys and liver showed high amount of radioactivity that attributed to the excretion ways. With respect to this biodistribution, [^{99m}Tc](HYNIC-AF7P)(tricine)(TPPTS) had good ability for tumor visualization, as the tumor was visible between 0.5 to 2 h p.i. This tumor visualization was specific and not only disappeared in the presence of excess non-labeled AF7P but also did not seen for negative MT1-MMP A-549 cancer cell line. Although [^{99m}Tc]-(HYNIC-AF7P)(tricine)(TPPTS) has good ability for specific targeting of MT1-MMP tumors, but for clinical practice it is necessary that the pharmacokinetic of a peptide including non-target accumulation was improved.

1.12. ^{131}I, ^{111}In, ^{99m}Tc-FROP-1 peptide

Zitzmann et al., used a phage peptide library to identify a new 12-amino-acid peptide (FROP-1) that was able to bind to thyroid carcinoma [162]. This peptide was highly attractive for diagnostic or therapeutic applications for follicular thyroid carcinoma cells. FROP-1 peptide had significantly binding to the various type of the cancer cell lines, especially thyroid cancer cells FRO82-2 and MCF-7 breast cancer cells. The binding kinetic of FROP-1 to MCF-7 cells was different from FRO82-2 cells. The IC_{50} values of (^{131}I, ^{125}I)-FROP-1 peptide for MCF-7 and FRO82-2 were found 12 μM and 8 μM, respectively. Biodistribution of ^{131}I-FROP-1 into female nu/nu mice bearing human thyroid tumors (FRO82-2) or human mammary carcinoma (MCF-7) showed maximum tumor uptake at 45 min p.i. The tumor-to-muscle ratios for FRO82-2

and MCF-7 tumors were found 4.8 and 7.9 after 135 min injection of ^{131}I-FROP-1 into mice, respectively. Despite the high FROP-1 peptide ability for detection of various cancer cell lines, this ability was non-efficient due to the slow binding kinetics (for FRO82-2 cell line) and low binding capacity (for other cancer cell lines). On the other hand, due to the peptide instability, the *in vivo* tumor uptake was low. In another study, Mier et al., investigated the influence of the chelator conjugation with FROP-1 peptide on binding and tumor uptake [163]. Serum stability results showed that ^{111}In-FROPDOTA is more stable than ^{131}I-FROP as; full-length peptide was still left after 120 min of incubation. FROPDOTA revealed different cellular uptake kinetics, reaching a maximum at 2 h that was slower than FROP-1. This binding (IC_{50} = 494 nM for FRO82-2 cell line) could be almost completely blocked in the presence of non-labeled FROP-1 as competitor, and also no binding was observed either for FROPDOTA or for FROP-1 for the non-tumor HPV-16GM and HUVEC cell lines. Biodistribution of FROPDOTA showed that ^{111}In-FROPDOTA reached a maximum tumor uptake (for both FRO82-2 and MCF-7) after 5 min postinjection and then radioactivity was decreased up to 45 min. In comparison to the FROP-1, the attachment of the chelator led to the fast blood clearance that did not allow the peptide to reach its maximum binding capacity. This rapid clearance is main reason of high kidney radioactivity and is caused by the hydrophilic DOTA conjugate. For coverage, this insufficient tumor uptake, in another study Mier et al., proposed the derivatives with prolonged circulation time (FROP-DOTA-PEG) [164]. However, positive effect of PEGylation including a substantially improved stabilization in the circulation led to stable tumor accumulation, unfortunately, according to the *in vitro* results, the PEGylated conjugate showed even slower binding kinetics than FROPDOTA. PEGylation of FROPDOTA decreased the fast washout of FROPDOTA from blood circulation, but effective tumor accumulation was found in delayed time point (Table 1).

With notice that the nature and location of a chelating moiety within a peptide molecule can influence on its receptor-binding, in another study our research group proposed the variation of DOTA chelator with HYNIC, to change tumor targeting characteristics of FROP-1 peptide and reached suitable tumor targeting. Therefor we radiolabeled FROP-1 peptide through practicing HYNIC as a chelating moiety (at the C-terminus) and Lys residue as a spacer in order to develop a ^{99m}Tc-HYNIC-(tricine/EDDA) for targeting and imaging of MCF-7 cancer cells [55]. The main reasons for this modification were including well-defined chemistry, post conjugation labeling, change radiolabeling process and forming a stable complex with ^{99m}Tc. High *in vitro* stability was found for ^{99m}Tc-HYNIC-(tricine/EDDA), that was stable up to 6 h in normal saline and 1 h in human plasma serum. The maximum binding capacity was found for MCF-7 cancer cells that this binding was specific with $K_D = 158 \pm 41$ nM and $B_{max} = 4.5 \pm 0.6 \times 10^7$ sites per cell. ^{99m}Tc-HYNIC-(tricine/EDDA) showed fast internalization rate however, maximum internalization was found after 6 h post incubation. Similar to ^{111}In-DOTA-FROP, the specific cell binding of ^{99m}Tc-HYNIC-FROP was not altered by the labeling with ^{99m}Tc. ^{99m}Tc-HYNIC-FROP exhibited a rapid clearance from the blood circulation that excretion pathway was mainly through renal system. The maximum uptake values of ^{99m}Tc-HYNIC-FROP in MCF-7 tumors was found after 30 min p.i. also the maximum tumor/muscle ratio was obtained after 15 min p.i. In comparison to the ^{131}I–FROP-1 and ^{111}In-DOTA-FROP, the modification of our proposed molecule was leading to not only the improvement of binding capacity and binding kinetics but also the *in vivo* tumor accumulation. Unfortunately, according to the biodistribution results ^{99m}Tc-HYNIC-FROP peptide has low tumor uptake than lung and heart, which is a limiting factor for imaging of breast cancer. Therefore, for investigation the type of co-ligand at FROP-1 targeting characterization and also obtaining better tumor uptake, the changing of co-ligand was proposed by our research group [54]. The main reason for changing the type of a co-ligand was that the radiolabeling with Tricine was performed at room temperature and not required to any heating for completing the radiolabeling reaction [104]. Approximately ^{99m}Tc-HYNIC-(tricine/EDDA)-FROP and ^{99m}Tc-HYNIC-(tricine)-FROP showed similar *in vitro* and *in vivo* results and the changing of co-ligand did not efficiently improve tumor uptake of this radiolabeled peptide.

1.13. ^{111}In-A20FMDV2 peptide for $\alpha_v\beta_6$ positive breast tumor

Integrin $\alpha_v\beta_6$ is mainly expressed on epithelial tissue. It is involved in wound healing, chronic inflammation of some normal tissues. It is overexpressed in cancer and can serve as a target for imaging and therapy [165–167]. The overexpression of integrin $\alpha_v\beta_6$ was reported in various cancers including squamous carcinoma, cervix, non-small cell lung cancer and colon cancer [168–173]. A 20-mer peptide, A20FMDV2 (NAVPNLRGDLQVLAQKVART), was derived from the VP1 coat protein that has specific and potent binding to $\alpha_v\beta_6$ [174,175]. This peptide was radiolabeled with ^{18}F and was used for non-invasive PET imaging that discriminated between β6-non-expressing and β6-expressing human xenografts [176]. In the next study, DOTA chelator was attached to this peptide and radiolabeled with ^{111}In radionuclide for *in vitro* and *in vivo* evaluations in A375Pβ6 (positive integrin $\alpha_v\beta_6$) and A375Ppuro (negative integrin $\alpha_v\beta_6$) cell lines. According to the flow cytometry, DTPA-A20FMDV2 bound only to positive integrin $\alpha_v\beta_6$ cell line and this binding not only specific but also was retained by addition of DOTA chelator. ^{111}In-DTPA-A20FMDV2 exhibited good stability as in phosphate buffer saline and in mouse serum, it was intact 50% of radiolabeled peptide after 4 h incubation. The affinity of radiolabeled peptide to A375Pβ6 was 1.73 ± 0.46 nM that was not seen any affinity on A375Ppuro negative cell line. The maximum internalization of ^{111}In-DTPA-A20FMDV2 was found after 1 h (89%–96%) and the absence of this internalization for A375Ppuro negative cell line confirmed specific internalization for this radiolabeled peptide. Also this internalization was not affected by DTPA as similar data that were obtained with biotinylated A20FMDV2. The *in vivo* evaluation of radiolabeled peptide demonstrated the specific tumor uptake for $\alpha_v\beta_6$6 positive tumor. According to the *in vivo* results, the accumulation of ^{111}In-DTPA-A20FMDV2 in the A375Pβ6 tumor was specific and higher than A375Ppuro tumor (7: 1). The T/B and T/M ratios were found 9 and 7 at 1 h p.i, respectively. The high amount of accumulations in non-target organs were observed in gallbladder, stomach, and descending GI tract, that are revealed to the overexpression of endogenous $\alpha_v\beta_6$. High accumulation of radioactivity in kidneys that not overexpress $\alpha_v\beta_6$, demonstrated that this accumulation was not mediated by $\alpha_v\beta_6$ receptor. On the other hand, the significant reduction of tumor accumulation in the presence of non-labeled DTPA-A20FMDV2 confirmed the specific tumor uptake for radiolabeled peptide which was mediated by $\alpha_v\beta_6$ receptor. Also the non-labeled peptide reduced uptake in the kidneys by more than 50%. The results of SPECT imaging of $\alpha_v\beta_6$6-expressing tumor demonstrated this radiolabeled peptide had good ability for visualization of $\alpha_v\beta_6$-positive $\alpha_v\beta_6$ positive human xenografts and corresponds closely to the biodistribution results. The ability of ^{111}In-DTPA-A20FMDV2 for visualization of $\alpha_v\beta_6$ receptor positive breast tumor was confirmed using of SPECT imaging in MCF10A.DCIS.COM and MCF10A.CA1a breast carcinoma cell lines with high overexpression of $\alpha_v\beta_6$ receptor [175,177]. The selective tumor uptake than non-target organ such as muscle (T/M = 15) was achieved and led to high tumor contrast for both breast tumor xenografts. In summary, ^{111}In-DTPA-A20FMDV2 locates specifically to$\alpha_v\beta_6$-expressing tissues *in vivo* and can be used for efficient imaging of $\alpha_v\beta_6$-expressing cancers especially for breast cancer that overexpress $\alpha_v\beta_6$ endogenously.

1.14. ^{99m}Tc- CLKADKAKC (CK3) as a neuropilin-1-targeting peptide for breast cancer targeting

Neuropilin-1 (NRP-1) is a multifunctional membrane receptor and numerates as a co-receptor of vascular endothelial growth factor

(VEGF) family [178–180]. NRP-1 is expressed in normal cells but well documented that the overexpression of NRP-1 has main role in initiation, growth, angiogenesis, invasion and metastasis of various tumors and in the case of breast tumor NRP-1 numerates as a multifunctional protein that is involved in angiogenesis and invasion [181–183]. NRP-1 is an attractive target for imaging and therapy of various cancers [184–186]. CK3 peptide was identified by phage library screening method and has potential for SPECT and NIRF imaging of MDA-MB-231 breast cancer cells with NRP-1 overexpression [187]. CK3 peptide showed high capacity binding to MDA-MB-231 breast cancer cells as compared to other breast cancer cells such as 4T-1, MDA-MB-435 and MCF-7. This binding mainly related to the expression of NRP-1 on the cells. The *in vivo* evaluation of ^{99m}Tc-labeled CK3 showed maximum accumulation in the aorta and kidneys after 20 min and 50 min p.i., respectively. The maximum tumor uptake was observed after 4 h p.i. Previously, several NRP-1-targeting peptides containing motif (RXRR) were identified by phage display. Although these peptides bound to NRP-1-positive cancer cells, but they penetrated and accumulated into the first encountered organ such as lung and heart [184,186]. In the case of CK3 peptide, accumulation in the lungs and heart was not seen. Similar to iRGD peptide as representative NRP-1 targeting peptide [188], ^{99m}Tc-CK3 peptide accumulated in tumor and could be used for imaging of breast cancer. ^{99m}Tc-CK3 showed good ability for visualization of MDA-MB-231 breast tumor with high contrast in SPECT image. The maximum accumulation was seen for kidneys that attributed to the exertion of radiolabeled peptide. Therefore, ^{99m}Tc-CK3 can been used for breast cancer imaging *in vivo*.

1.15. ^{111}In-A9 peptide for HER2 positive breast cancer

Recently, several trastuzumab-Fab derived peptides have been developed for HER2 overexpression targeting in cancers [189–191]. A9 nonapeptide (WAVQNTDAV) showed nanomolar affinity to HER2-receptor and also putative internalization inside the cells. The site-specific conjugation of DTPA chelator to the N-terminus of A9 peptide and radiolabeling with ^{111}In were conducted for non-invasive imaging of HER2-expression level in metastases BT474 breast cancer cells [192]. No measurable release of radioactivity was seen after incubation of ^{111}In-DTPA-A9 with murine plasma after 60 min that was demonstrated good *in vivo* stability against peptidases. According to the interaction Map of ^{111}In-DTPA-A9 with HER2-expressing BT474 cells, the binding of radiolabeled peptide is mediated by two binding sites, one strong, with affinity of 4.9 nM, and one weaker, with affinity 103 nM that might be attributed to homo- and heterodimerization of receptors on cancer cells. It is interesting to mention that high affinity interaction was nearly completely suppressed, upon traztuzumab displacement, while low affinity interaction remained. One of these interactions is HER2-specific that be suppressed by trastuzumab, however another is non-HER2 specific and might be characteristic for peptide. It was observed that the affinity in a single digit nanomolar range was required for efficient targeting of tumors with high HER2 expression [193]. Similar phenomenon has been found earlier for binding of ^{125}I-labeled anti-HER2 antibody trastuzumab and ^{111}In-labeled anti-HER2 affibody molecules to different HER2-expressing cells [194]. According to the *in vivo* results in normal mice, ^{111}In-DTPA-A9 showed undesirable accumulation in normal tissues at 1 h after injection that may attribute to the weak non-HER2-specific interaction. The low radioactivity in the gastrointestinal tract is attributed to the exertion of radiolabeled peptide from hepatobiliary exertion. Maximum accumulation of radioactivity was found for kidneys that may related to the renal excretion with subsequent tubular reabsorption. ^{111}In-DTPA-A9 rapidly cleared from blood circulation and has sufficient *in vivo* stability that may offer good tumor imaging with high contrast. Although the biodistribution of this peptide in HER2 positive tumor cancer cell engrafted in nude mice is required for more evaluation of targeting and imaging ability.

1.16. ^{131}I-labeled p160 peptide for keratin 1 receptor

Linear dodecapeptide p160 (VPWMEPAYQRFL) as breast cancer cell-binding peptide was firstly identified through random peptide phage display with specificity for the breast cancer cell line MDA-MB-435 and the neuroblastoma cell line WAC 2 [195,196]. Peptide p160 displays strong bound not only to MDA-MB-435 but also to MCF-7 breast cancer cells with minimal binding to normal human umbilical vein endothelial cells (HUVECs) [197]. Also one analogue of p160 namely 18–4 (WxEAAYQrFL) was developed in comparison to p160 that was resistance to proteolysis in biological fluids such as human serum and liver homogenate. Similar to p160 peptide, its analogue was able to bind breast cancer cell surface receptors and rapidly internalized to cells via endocytosis. Due to the ability specific binding to MDA-MB-435 breast cancer cell, 18–4 peptide was used for targeted therapy of nude mice bearing MDA-MB-435 and human mammary epithelial MCF-10A xenografts that received peptide 18–4 conjugated liposomal doxorubicin (Dox) [198,199]. The finding target of p160 peptide was conducted and the results confirmed that 67 kDa keratin-1 (KRT1) is the target receptor for p160 peptide and its analogue [200]. KRT1 receptor is overexpressed in some cancer cells, such as MCF-7 and MDA-MB-435, however its expression in normal mammary epithelial cells such as MCF-10A is low [201–204]. The overexpression of KRT1 receptor in these cancer cell lines can be responsible for the specific and enhanced uptake of p160 peptide. The K_D values for p160 and 18–4 peptide were calculated to be 1.1 μM and 0.98 μM, respectively. ^{125}I-labeled p160 peptide showed maximum binding capacity to MCF-7 and also significant binding to MDA-MD-435 cells. This binding was specific and mediated by receptor as, in the presence of excess non-labeled p160 peptide, the binding was significantly blocked, whereas it was not blocked by octreotide. The low amount of binding was seen for HUVEC cells and was not competitively abolished by the non-labeled p160 peptide as competitor. According to competition experiment, the IC_{50}, K_D and B_{max} values were found 0.6 ± 0.9 μmol/L, 0.86 μmol/L and 1.03×10^{11} sites per cell, respectively. High B_{max} value can offer better recognition of target on cancer cell surface and leads to better *in vivo* tumor visualization. The maximum internalization of radiolabeled peptide into the MDA-MB-435 cells was occurred after 1 h incubation and mainly suppressed in the presence of excess competitor. ^{125}I-labeled p160 peptide showed fast blood degradation by serum proteases and after 1 h, full length peptide completely was degraded. The *in vivo* evaluation of ^{131}I-labeled p160 peptide in female nude mice bearing human breast cancer MDA-MB-435 tumors after 1 h p.i, showed fast tumor uptake that was higher than in heart, spleen, liver, and brain and almost the same compared with the kidneys. Unfortunately, blood activity was higher than tumor that may reduce contrast for breast imaging. High blood accumulation may have attributed to the interaction of p160 peptide with serum proteins such as albumin and *in vivo* instability. In the case of lung tissue, the accumulated activity approximately was same with tumor, however perfusion experiment led to the decrease of radioactivity in lung tissue whereas the uptake in the tumor remained almost constant. Therefore, this experiment demonstrated the nonspecific uptake for non-target tissue was mainly mediated by blood pool. In the case of p160 peptide, one major issue that is required for improving the pharmacokinetics of peptide at further investigation is the stabilization of p160 peptide for example cyclization and especially using bifunctional chelating agent such as HYNIC. It's necessary to mention that the addition of polar spacer may improve the clearance of a peptide from blood circulation and also may reduce the interaction of peptide with serum proteins. With notice that the same biodistribution results was seen for ^{131}I-FITC-RGD-4C in nude mice bearing MDA-MB-435 breast cancer tumors and also a prerequisite for the use of an agent as *in vivo* imaging agent such as selective binding to the tumor tissue with low uptake by normal tissues especially lungs and heart, ^{131}I-labeled p160 peptide can be served as suitable breast cancer imaging agent in clinical practice.

Table 2
Challenges of radiolabeled peptides for breast imaging.

Challenge	Results
In vivo instability	Low tumor uptake, highly background radioactivity, low blood clearance
Low affinity to target	Low tumor uptake, high non-targets uptakes, non-contrast in tumor imaging
High non-target tissues uptakes	Non-contrast tumor imaging
High uptakes in lung, heart and nipple	Low contrast tumor imaging, non-diagnosis primary tumor and metastasis
Low blood clearance	High background radioactivity, low contrast in tumor imaging, delay in tumor imaging, not suitable for short live radionuclide
Liver uptake	Non-diagnosis the metastasis in abdominal
Kidneys retention	High radiation dose to kidneys, increased background radioactivity
Low tumor uptake and fast washout	Non-contrast tumor imaging
Slow pharmacokinetics binding accompanied with *in vivo* instability	Low tumor uptake, high burden radiation dose to non-target tissue and low contrast tumor imaging
Low internalization	Low tumor uptake

2. Conclusion

The rising incidence of breast cancer worldwide increases the importance of developing new molecular imaging agent for early diagnosis before tumor metastasis. Major challenge in this regard is developing to design high sensitive molecular imaging agent with high tumor contrast. Several evidences have demonstrated the overexpression tumor specific receptors in cancer cell surface according to the initiation and progression of tumor. In recent years' identification and targeting of these receptors with various molecular imaging agent is using as suitable tool for early detection of breast cancer. Among to the molecular imaging agent, peptides have superior and specific popularity according to the suitable pharmacokinetics and enormous potential applications. Small peptide radiolabeled with various radionuclide specially SPECT radionuclide provide effective approach for easy and low cost imaging and diagnosis of breast cancer for enhancing therapeutic efficacy. So far, different type of peptides with specific affinity binding to breast overexpressed receptors were developed and radiolabeled. According to the recent efforts of scientist for developing an ideal peptide base radiopharmaceutical for breast cancer, some identified peptides have good ability for targeting and imaging of breast cancer, however for using of these peptides in clinical care more efforts should have been carry out. Initially it is necessary that the identified peptide must have good affinity and avid binding to the overexpressed receptor in breast cancer cells. Then the radiolabeling process with suitable photonic characteristics radionuclide was simple and has good radiochemical purity without diminishing of a peptide binding to specific site. Due to the fast degradation of peptides by serum peptidase and renal degradation, the *in vivo* stability of peptide base radiopharmaceuticals is very important factor for sufficient in *vivo* tumor uptake. The sufficient tumor uptake especially at delayed time points that assemble good situation for imaging, because of low blood background, is restricted. Also, slow binding pharmacokinetic, which accompanied with *in vivo* instability leads to great failure for *in vivo* tumor imaging. Specific binding of radiolabeled peptide especially mediated via overexpressed receptors and high amounts of internalization are main requisites for imaging ability. As for these requisitions for radiolabeled peptide, several main *in vivo* features are necessary for tumor imaging are including fast clearance from blood circulation without any degradation and high specific and continuous tumor uptake at early time point after injection offer the excellent tumor imaging with high contrast. For some peptides, one or two of these characterizations was not existed. In the case of some peptides, fast washout from tumor tissue with passing the time is another problem that leads to failure for *in vivo* tumor imaging. If the peptide has continuous tumor uptake with passing the time but fast clearance from blood circulation obstacles for sufficient tumor uptake, the application of various methods that lead to the more retention of peptide in blood circulation may help to reach high *in vivo* tumor uptake. However, it is necessary that the non-target accumulation of radiolabeled peptide be considered as low when researchers have decided to use these modifications. Non-target accumulation especially in lungs and heart is very important factor for *in vivo* breast tumor imaging. If the peptide has high lungs and heart accumulation and also low or equal tumor accumulation with these organs, the imaging of breast tumors will be difficult. For other tumors, intestines uptake is important factor for visualization of tumor in abdominal area. The summarize of these challenges for breast cancer imaging with radiolabeled peptide are giving in Table 2. The new peptide which was developed for imaging of breast cancer may have one or even all of these deficiency. Using suitable modifications such as modification of peptide sequence and using suitable spacer or chelator, developing of a peptide which routinely was used for breast tumor imaging in clinical care be feasible.

Declaration of competing interest

The authors declare that there are no conflicts of interest.

References

[1] K. McPherson, C.M. Steel, J.M. Dixon, ABC of breast diseases. Breast cancer-epidemiology, risk factors, and genetics, BMJ (Clin. Res. ed) 321 (2000) 624–628.
[2] H. Liu, Y. Chen, S. Wu, F. Song, H. Zhang, M. Tian, Molecular imaging using PET and SPECT for identification of breast cancer subtypes, Nucl. Med. Commun. 37 (2016) 1116–1124.
[3] C.M. Perou, T. Sorlie, M.B. Eisen, M. van de Rijn, S.S. Jeffrey, C.A. Rees, et al., Molecular portraits of human breast tumours, Nature 406 (2000) 747–752.
[4] T. Sorlie, C.M. Perou, R. Tibshirani, T. Aas, S. Geisler, H. Johnsen, et al., Gene expression patterns of breast carcinomas distinguish tumor subclasses with clinical implications, Proc. Natl. Acad. Sci. U. S. A. 98 (2001) 10869–10874.
[5] T. Sorlie, R. Tibshirani, J. Parker, T. Hastie, J.S. Marron, A. Nobel, et al., Repeated observation of breast tumor subtypes in independent gene expression data sets, Proceedings of the National Academy of Sciences of the United States of America vol. 100, (2003), pp. 8418–8423.
[6] S. Winters, C. Martin, D. Murphy, N.K. Shokar, Breast cancer epidemiology, prevention, and screening, Prog. Mol. Biol. Transl. Sci. 151 (2017) 1–32.
[7] T. Hamaoka, J.E. Madewell, D.A. Podoloff, G.N. Hortobagyi, N.T. Ueno, Bone imaging in metastatic breast cancer, J. Clin. Oncol. : Off. J. Am. Soc. Clin. Oncol. 22 (2004) 2942–2953.
[8] G. Savelli, L. Maffioli, M. Maccauro, E. De Deckere, E. Bombardieri, Bone scintigraphy and the added value of SPECT (single photon emission tomography) in detecting skeletal lesions, Q. J. Nucl. Med. : Off. Publ. Ital. Assoc. Nucl. Med. (Aimn) Int. Assoc. Radiopharmacol. (Iar) 45 (2001) 27–37.
[9] S. Kosuda, T. Kaji, H. Yokoyama, T. Yokokawa, M. Katayama, T. Iriye, et al., Does bone SPECT actually have lower sensitivity for detecting vertebral metastasis than MRI? J. Nucl. Med. : Off. Publ. Soc. Nucl. Med. 37 (1996) 975–978.
[10] S. Ben-Haim, O. Israel, Breast cancer: role of SPECT and PET in imaging bone metastases, Semin. Nucl. Med. 39 (2009) 408–415.
[11] I.N. Nechaev, E.N. Knyazev, N.A. Krainova, M.Y. Shkurnikov, Express analysis of HER-2/neu status in breast cancer biopsy specimens, Bull. Exp. Biol. Med. 155 (2013) 522–526.
[12] J.L. Hsu, M.C. Hung, The role of HER2, EGFR, and other receptor tyrosine kinases in breast cancer, Cancer Metastasis Rev. 35 (2016) 575–588.
[13] R.S. Tolhurst, R.S. Thomas, F.J. Kyle, H. Patel, M. Periyasamy, A. Photiou, et al., Transient over-expression of estrogen receptor-alpha in breast cancer cells promotes cell survival and estrogen-independent growth, Breast Canc. Res. Treat. 128 (2011) 357–368.
[14] D.J. Buchsbaum, Imaging and therapy of tumors induced to express somatostatin receptor by gene transfer using radiolabeled peptides and single chain antibody constructs, Semin. Nucl. Med. 34 (2004) 32–46.
[15] J. Fichna, A. Janecka, Synthesis of target-specific radiolabeled peptides for

diagnostic imaging, Bioconjug. Chem. 14 (2003) 3–17.
[16] A.L. Vavere, R. Rossin, Molecular imaging of cancer with radiolabeled peptides and PET, Anti Cancer Agents Med. Chem. 12 (2012) 462–475.
[17] R.R. Warner, T.M. O'Dorisio, Radiolabeled peptides in diagnosis and tumor imaging: clinical overview, Semin. Nucl. Med. 32 (2002) 79–83.
[18] S.U. Dalm, W.A. Schrijver, A.M. Sieuwerts, M.P. Look, A.C. Ziel-van der Made, V. de Weerd, et al., Prospects of targeting the gastrin releasing peptide receptor and somatostatin receptor 2 for nuclear imaging and therapy in metastatic breast cancer, PLoS One 12 (2017) e0170536.
[19] Z. Kazemi, M.H. Zahmatkesh, S.M. Abedi, S.J. Hosseinimehr, Biological evaluation of 99mTc-HYNIC-EDDA/tricine-(Ser)-D4 peptide for tumor targeting, Curr. Radiopharm. 10 (2017) 123–130.
[20] F. Khodadust, S. Ahmadpour, N. Aligholikhamseh, S.M. Abedi, S.J. Hosseinimehr, An improved (99m)Tc-HYNIC-(Ser)3-LTVSPWY peptide with EDDA/tricine as co-ligands for targeting and imaging of HER2 overexpression tumor, Eur. J. Med. Chem. 144 (2018) 767–773.
[21] N. Rahmanian, S.J. Hosseinimehr, A. Khalaj, Z. Noaparast, S.M. Abedi, O. Sabzevari, (99m)Tc-radiolabeled GE11-modified peptide for ovarian tumor targeting, Daru : J. Fac. Pharm. Tehran Univ. Med. Sci. 25 (2017) 13.
[22] H. Sabahnoo, Z. Noaparast, S.M. Abedi, S.J. Hosseinimehr, New small (99m)Tc-labeled peptides for HER2 receptor imaging, Eur. J. Med. Chem. 127 (2017) 1012–1024.
[23] S.A. Torabizadeh, S.M. Abedi, Z. Noaparast, S.J. Hosseinimehr, Comparative assessment of a (99m)Tc labeled H1299.2-HYNIC peptide bearing two different co-ligands for tumor-targeted imaging, Bioorg. Med. Chem. 25 (2017) 2583–2592.
[24] A. Appert-Collin, P. Hubert, G. Cremel, A. Bennasroune, Role of ErbB receptors in cancer cell migration and invasion, Front. Pharmacol. 6 (2015) 283.
[25] M.A. Lemmon, J. Schlessinger, Cell signaling by receptor tyrosine kinases, Cell 141 (2010) 1117–1134.
[26] Y. Yarden, B.Z. Shilo, SnapShot: EGFR signaling pathway, Cell 131 (2007) 1018.
[27] Y. Yarden, M.X. Sliwkowski, Untangling the ErbB signalling network, Nat. Rev. Mol. Cell Biol. 2 (2001) 127–137.
[28] M.K. Chen, M.C. Hung, Proteolytic cleavage, trafficking, and functions of nuclear receptor tyrosine kinases, FEBS J. 282 (2015) 3693–3721.
[29] J. Baselga, S.M. Swain, Novel anticancer targets: revisiting ERBB2 and discovering ERBB3, Nat. Rev. Cancer 9 (2009) 463–475.
[30] N.E. Hynes, G. MacDonald, ErbB receptors and signaling pathways in cancer, Curr. Opin. Cell Biol. 21 (2009) 177–184.
[31] N. Prenzel, O.M. Fischer, S. Streit, S. Hart, A. Ullrich, The epidermal growth factor receptor family as a central element for cellular signal transduction and diversification, Endocr. Relat. Cancer 8 (2001) 11–31.
[32] P. Carter, L. Presta, C.M. Gorman, J.B. Ridgway, D. Henner, W.L. Wong, et al., Humanization of an anti-p185HER2 antibody for human cancer therapy, Proc. Natl. Acad. Sci. U. S. A. 89 (1992) 4285–4289.
[33] C.L. Arteaga, J.A. Engelman, ERBB receptors: from oncogene discovery to basic science to mechanism-based cancer therapeutics, Cancer Cell 25 (2014) 282–303.
[34] G.E. Konecny, M.D. Pegram, N. Venkatesan, R. Finn, G. Yang, M. Rahmeh, et al., Activity of the dual kinase inhibitor lapatinib (GW572016) against HER-2-overexpressing and trastuzumab-treated breast cancer cells, Cancer Res. 66 (2006) 1630–1639.
[35] G.D. Lewis Phillips, G. Li, D.L. Dugger, L.M. Crocker, K.L. Parsons, E. Mai, et al., Targeting HER2-positive breast cancer with trastuzumab-DM1, an antibody-cytotoxic drug conjugate, Cancer Res. 68 (2008) 9280–9290.
[36] G. Lurje, H.J. Lenz, EGFR signaling and drug discovery, Oncology 77 (2009) 400–410.
[37] J.R. Sainsbury, J.R. Farndon, G.K. Needham, A.J. Malcolm, A.L. Harris, Epidermal-growth-factor receptor status as predictor of early recurrence of and death from breast cancer, Lancet (London, England) 1 (1987) 1398–1402.
[38] S. Tsutsui, S. Ohno, S. Murakami, Y. Hachitanda, S. Oda, Prognostic value of epidermal growth factor receptor (EGFR) and its relationship to the estrogen receptor status in 1029 patients with breast cancer, Breast Canc. Res. Treat. 71 (2002) 67–75.
[39] C.J. Witton, J.R. Reeves, J.J. Going, T.G. Cooke, J.M. Bartlett, Expression of the HER1-4 family of receptor tyrosine kinases in breast cancer, J. Pathol. 200 (2003) 290–297.
[40] R. Bhargava, W.L. Gerald, A.R. Li, Q. Pan, P. Lal, M. Ladanyi, et al., EGFR gene amplification in breast cancer: correlation with epidermal growth factor receptor mRNA and protein expression and HER-2 status and absence of EGFR-activating mutations, Mod. Pathol. : Off. J. U. S. Can. Acad. Pathol. Inc. 18 (2005) 1027–1033.
[41] B.D. Lehmann, J.A. Bauer, X. Chen, M.E. Sanders, A.B. Chakravarthy, Y. Shyr, et al., Identification of human triple-negative breast cancer subtypes and preclinical models for selection of targeted therapies, J. Clin. Investig. 121 (2011) 2750–2767.
[42] H. Masuda, D. Zhang, C. Bartholomeusz, H. Doihara, G.N. Hortobagyi, N.T. Ueno, Role of epidermal growth factor receptor in breast cancer, Breast Canc. Res. Treat. 136 (2012) 331–345.
[43] E.A. Rakha, M.E. El-Sayed, A.R. Green, A.H. Lee, J.F. Robertson, I.O. Ellis, Prognostic markers in triple-negative breast cancer, Cancer 109 (2007) 25–32.
[44] J.S. Reis-Filho, C. Pinheiro, M.B. Lambros, F. Milanezi, S. Carvalho, K. Savage, et al., EGFR amplification and lack of activating mutations in metaplastic breast carcinomas, J. Pathol. 209 (2006) 445–453.
[45] S.Y. Park, J.H. Choi, J.S. Nam, Targeting cancer stem cells in triple-negative breast cancer, Cancers 11 (2019).
[46] T. Saha, S. Makar, R. Swetha, G. Gutti, S.K. Singh, Estrogen signaling: an emanating therapeutic target for breast cancer treatment, Eur. J. Med. Chem. 177 (2019) 116–143.
[47] D. Sharma, S. Kumar, B. Narasimhan, Estrogen alpha receptor antagonists for the treatment of breast cancer: a review, Chem. Cent. J. 12 (2018) 107.
[48] M. Cameron Smith, C. Orlando, M. Serio, M. Maggi, Somatostatin receptors and breast cancer, J. Endocrinol. Investig. 26 (2003) 125–130.
[49] F.J. Gomez-de la Fuente, J. Jimenez-Bonilla, J. Estevez, I. Martinez-Rodriguez, I. Banzo, Somatostatin receptors expression in breast cancer, Cir. Esp. 95 (2017) 545–547.
[50] W.H. Bakker, E.P. Krenning, W.A. Breeman, J.W. Koper, P.P. Kooij, J.C. Reubi, et al., Receptor scintigraphy with a radioiodinated somatostatin analogue: radiolabeling, purification, biologic activity, and in vivo application in animals, J. Nucl. Med. : Off. Publ. Soc. Nucl. Med. 31 (1990) 1501–1509.
[51] K. De, A. Bhowmik, A. Behera, I. Banerjee, M.K. Ghosh, M. Misra, Synthesis, radiolabeling, and preclinical evaluation of a new octreotide analog for somatostatin receptor-positive tumor scintigraphy, J. Pept. Sci. : Off. Publ. Europ. Pept. Soc. 18 (2012) 720–730.
[52] C.J. Smith, G.L. Sieckman, N.K. Owen, D.L. Hayes, D.G. Mazuru, R. Kannan, et al., Radiochemical investigations of gastrin-releasing peptide receptor-specific [(99m)Tc(X)(CO)3-Dpr-Ser-Ser-Ser-Gln-Trp-Ala-Val-Gly-His-Leu-Met-(NH2)] in PC-3, tumor-bearing, rodent models: syntheses, radiolabeling, and in vitro/in vivo studies where Dpr = 2,3-diaminopropionic acid and X = H2O or P(CH2OH)3, Cancer Res. 63 (2003) 4082–4088.
[53] C. Morgat, R. Schollhammer, G. Macgrogan, N. Barthe, V. Velasco, D. Vimont, et al., Comparison of the binding of the gastrin-releasing peptide receptor (GRP-R) antagonist 68Ga-RM2 and 18F-FDG in breast cancer samples, PLoS One 14 (2019) e0210905.
[54] S. Ahmadpour, Z. Noaparast, S.M. Abedi, S.J. Hosseinimehr, (99m)Tc-(tricine)-HYNIC-Lys-FROP peptide for breast tumor targeting, Anti Cancer Agents Med. Chem. 18 (2018) 1295–1302.
[55] S. Ahmadpour, Z. Noaparast, S.M. Abedi, S.J. Hosseinimehr, (99m)Tc-HYNIC-(tricine/EDDA)-FROP peptide for MCF-7 breast tumor targeting and imaging, J. Biomed. Sci. 25 (2018) 17.
[56] M. Piramoon, S.J. Hosseinimehr, K. Omidfar, Z. Noaparast, S.M. Abedi, (99m) Tc-anti-epidermal growth factor receptor nanobody for tumor imaging, Chem. Biol. Drug Des. 89 (2017) 498–504.
[57] H.J. Kim, J.Y. Park, T.S. Lee, I.H. Song, Y.L. Cho, J.R. Chae, et al., PET imaging of HER2 expression with an 18F-fluoride labeled aptamer, PLoS One 14 (2019) e0211047.
[58] K. Varmira, S.J. Hosseinimehr, Z. Noaparast, S.M. Abedi, A HER2-targeted RNA aptamer molecule labeled with 99mTc for single-photon imaging in malignant tumors, Nucl. Med. Biol. 40 (2013) 980–986.
[59] K. Varmira, S.J. Hosseinimehr, Z. Noaparast, S.M. Abedi, An improved radiolabelled RNA aptamer molecule for HER2 imaging in cancers, J. Drug Target. 22 (2014) 116–122.
[60] A.Z. Wang, O.C. Farokhzad, Current progress of aptamer-based molecular imaging, J. Nucl. Med. : Off. Publ. Soc. Nucl. Med. 55 (2014) 353–356.
[61] J.W. Hicks, H.F. VanBrocklin, A.A. Wilson, S. Houle, N. Vasdev, Radiolabeled small molecule protein kinase inhibitors for imaging with PET or SPECT, Molecules 15 (2010) 8260–8278.
[62] L. Tang, C. Peng, B. Tang, Z. Li, X. Wang, J. Li, et al., Radioiodinated small-molecule tyrosine kinase inhibitor for HER2-selective SPECT imaging, J. Nucl. Med. : Off. Publ. Soc. Nucl. Med. 59 (2018) 1386–1391.
[63] D. Blok, R.I. Feitsma, P. Vermeij, E.J. Pauwels, Peptide radiopharmaceuticals in nuclear medicine, Eur. J. Nucl. Med. 26 (1999) 1511–1519.
[64] S.M. Okarvi, Recent developments in 99Tcm-labelled peptide-based radiopharmaceuticals: an overview, Nucl. Med. Commun. 20 (1999) 1093–1112.
[65] S.M. Okarvi, Peptide-based radiopharmaceuticals: future tools for diagnostic imaging of cancers and other diseases, Med. Res. Rev. 24 (2004) 357–397.
[66] J.G. McAfee, R.D. Neumann, Radiolabeled peptides and other ligands for receptors overexpressed in tumor cells for imaging neoplasms, Nucl. Med. Biol. 23 (1996) 673–676.
[67] S.U. Dalm, J.F. Verzijlbergen, M. De Jong, Review: receptor targeted nuclear imaging of breast cancer, Int. J. Mol. Sci. 18 (2017).
[68] S.U. Dalm, M. Melis, J. Emmering, D.J. Kwekkeboom, M. de Jong, Breast cancer imaging using radiolabelled somatostatin analogues, Nucl. Med. Biol. 43 (2016) 559–565.
[69] T.W. Moody, I. Gozes, Vasoactive intestinal peptide receptors: a molecular target in breast and lung cancer, Curr. Pharmaceut. Des. 13 (2007) 1099–1104.
[70] R. Bam, M. Laffey, K. Nottberg, P.S. Lown, B.J. Hackel, K.E. Wilson, Affibody-indocyanine green based contrast agent for photoacoustic and fluorescence molecular imaging of B7-H3 expression in breast cancer, Bioconjug. Chem. 30 (2019) 1677–1689.
[71] R.P. Baum, V. Prasad, D. Muller, C. Schuchardt, A. Orlova, A. Wennborg, et al., Molecular imaging of HER2-expressing malignant tumors in breast cancer patients using synthetic 111In- or 68Ga-labeled affibody molecules, J. Nucl. Med. : Off. Publ. Soc. Nucl. Med. 51 (2010) 892–897.
[72] A. De, G. Kuppusamy, V. Karri, Affibody molecules for molecular imaging and targeted drug delivery in the management of breast cancer, Int. J. Biol. Macromol. 107 (2018) 906–919.
[73] J. Sorensen, D. Sandberg, M. Sandstrom, A. Wennborg, J. Feldwisch, V. Tolmachev, et al., First-in-human molecular imaging of HER2 expression in breast cancer metastases using the 111In-ABY-025 affibody molecule, J. Nucl. Med. : Off. Publ. Soc. Nucl. Med. 55 (2014) 730–735.
[74] R. Chakravarty, S. Chakraborty, A. Dash, Molecular imaging of breast cancer: role of RGD peptides, Mini Rev. Med. Chem. 15 (2015) 1073–1094.
[75] F. Scopinaro, A. Varvarigou, W. Ussof, G. De Vincentis, S. Archimandritis,

G. Evangelatos, et al., Breast cancer takes up 99mTc bombesin. A preliminary report, Tumori 88 (2002) S25–S28.
[76] D.R. Bard, C.G. Knight, D.P. Page-Thomas, A chelating derivative of alpha-melanocyte stimulating hormone as a potential imaging agent for malignant melanoma, Br. J. Canc. 62 (1990) 919–922.
[77] M.F. Powell, H. Grey, F. Gaeta, A. Sette, S. Colon, Peptide stability in drug development: a comparison of peptide reactivity in different biological media, J. Pharm. Sci. 81 (1992) 731–735.
[78] R.E. Weiner, M.L. Thakur, Radiolabeled peptides in diagnosis and therapy, Semin. Nucl. Med. 31 (2001) 296–311.
[79] S. Ahmadpour, S.J. Hosseinimehr, PASylation as a powerful technology for improving the pharmacokinetic properties of biopharmaceuticals, Curr. Drug Deliv. 15 (2018) 331–341.
[80] G. Mariani, L. Bruselli, A. Duatti, Is PET always an advantage versus planar and SPECT imaging? Eur. J. Nucl. Med. Mol. Imaging 35 (2008) 1560–1565.
[81] H.N. Wagner Jr., From molecular imaging to molecular medicine, J. Nucl. Med. : Off. Publ. Soc. Nucl. Med. 47 (2006) 13N-5N, 7N-21N, 2N-6N passim.
[82] S. Chattopadhyay, S. Saha Das, L. Barua, A.K. Pal, U. Kumar, Madhusmita, et al., A Compact Solvent Extraction Based (99)Mo/(99)(m)Tc Generator for Hospital Radiopharmacy. Applied Radiation and Isotopes : Including Data, Instrumentation and Methods for Use in Agriculture, Industry and Medicine vol. 143, (2019), pp. 41–46.
[83] V.P. Chechev, M.M. Be, Radioactive equilibrium: 99Mo/99mTc decay characteristics, Appl. Radiat. Isot. : Incl. Data Instrum. Methods Use Agric. Ind. Med. 87 (2014) 132–136.
[84] W.W. Lee, Clinical applications of technetium-99m quantitative single-photon emission computed tomography/computed tomography, Nuc. Med. Mol. Imag. 53 (2019) 172–181.
[85] D. Papagiannopoulou, Technetium-99m radiochemistry for pharmaceutical applications, J. Label. Comp. Radiopharm. 60 (2017) 502–520.
[86] R. Piva, F. Ticconi, V. Ceriani, F. Scalorbi, F. Fiz, S. Capitanio, et al., Comparative Diagnostic Accuracy of 18F-FDG PET/CT for Breast Cancer Recurrence. Breast Cancer vol. 9, Dove Medical Press), 2017, pp. 461–471.
[87] T. Suzuki, K. Uno, A. Kubo, [Usefulness of 18F-FDG PET in the diagnosis for breast cancer patients], Nihon Rinsho Jap. J. Clin. Med. 64 (2006) 504–510.
[88] K. Tayama, U. Toh, T. Fujii, K. Shirouzu, Y. Kaida, [Usefulness of 18F-FDG-PET in breast cancer imaging], Nihon Rinsho Jap. J. Clin. Med. 65 (Suppl 6) (2007) 373–378.
[89] E. Ambrus, K. Ormandi, T. Sera, A. Toszegi, L. Csernay, L. Pavics, [The role of 99mTc-MIBI mammoscintigraphy in the diagnosis of breast cancer], Orv. Hetil. 139 (1998) 183–187.
[90] S. Del Vecchio, M. Salvatore, 99mTc-MIBI in the evaluation of breast cancer biology, Eur. J. Nucl. Med. Mol. Imaging 31 (Suppl 1) (2004) S88–S96.
[91] A. Zhang, P. Li, Q. Liu, S. Song, Breast-specific gamma camera imaging with (99m)Tc-MIBI has better diagnostic performance than magnetic resonance imaging in breast cancer patients: a meta-analysis, Hellenic J. Nucl. Med. 20 (2017) 26–35.
[92] M. Hagenauer, E.B. Silberstein, Detection of clinically occult axillary metastases from breast cancer during stress TI-201 scintigraphy, Clin. Nucl. Med. 16 (1991) 520.
[93] V.W. Lee, E.J. Sax, D.B. McAneny, S. Pollack, R.A. Blanchard, R.M. Beazley, et al., A complementary role for thallium-201 scintigraphy with mammography in the diagnosis of breast cancer, J. Nucl. Med. : Off. Publ. Soc. Nucl. Med. 34 (1993) 2095–2100.
[94] Z. Wang, W. Wang, X. Bu, Z. Wei, L. Geng, Y. Wu, et al., Microarray based screening of peptide nano probes for HER2 positive tumor, Anal. Chem. 87 (2015) 8367–8372.
[95] L. Li, Y. Wu, Z. Wang, B. Jia, Z. Hu, C. Dong, et al., SPECT/CT imaging of the novel HER2-targeted peptide probe (99m)Tc-HYNIC-H6F in breast cancer mouse models, J. Nucl. Med. : Off. Publ. Soc. Nucl. Med. 58 (2017) 821–826.
[96] U. Brown-Glaberman, Z. Dayao, M. Royce, HER2-targeted therapy for early-stage breast cancer: a comprehensive review, Oncology (Williston Park, NY) 28 (2014) 281–289.
[97] T. Fujita, H. Doihara, K. Kawasaki, D. Takabatake, H. Takahashi, K. Washio, et al., PTEN activity could be a predictive marker of trastuzumab efficacy in the treatment of ErbB2-overexpressing breast cancer, Br. J. Canc. 94 (2006) 247–252.
[98] R. Nahta, F.J. Esteva, Trastuzumab: triumphs and tribulations, Oncogene 26 (2007) 3637–3643.
[99] E.A. Mittendorf, Y. Wu, M. Scaltriti, F. Meric-Bernstam, K.K. Hunt, S. Dawood, et al., Loss of HER2 amplification following trastuzumab-based neoadjuvant systemic therapy and survival outcomes, Clin. Cancer Res. : Off. J. Am. Assoc. Canc. Res. 15 (2009) 7381–7388.
[100] G.B. Sivolapenko, V. Douli, D. Pectasides, D. Skarlos, G. Sirmalis, R. Hussain, et al., Breast cancer imaging with radiolabelled peptide from complementarity-determining region of antitumour antibody, Lancet (London, England) 346 (1995) 1662–1666.
[101] R. Hussain, N.S. Courtenay-Luck, G. Siligardi, Structure-function correlation and biostability of antibody CDR-derived peptides as tumour imaging agents, Biomed. Peptides, Proteins & Nucleic acids Struct. Synth. Biol. Act. 2 (1996) 67–70.
[102] S.M. Okarvi, Synthesis, radiolabeling and in vitro and in vivo characterization of a technetium-99m-labeled alpha-M2 peptide as a tumor imaging agent, J. Pept. Res. : Off. J. Am. Pept. Soc. 63 (2004) 460–468.
[103] W.C. Eckelman, J. Steigman, Direct labeling with 99mTc, Int. J. Radiat. Appl. Instrum. Part B Nucl. Med. Biol. 18 (1991) 3–7.
[104] S.A. Torabizadeh, S.J. Hosseinimehr, The influence of Co-ligands on improving tumor targeting of ^{99m}tc-HYNIC conjugated peptides, Mini Rev. Med. Chem. 17 (2017) 86–94.
[105] Y. Wang, G. Liu, D.J. Hnatowich, Methods for MAG3 conjugation and 99mTc radiolabeling of biomolecules, Nat. Protoc. 1 (2006) 1477–1480.
[106] C. Zhang, T.Z. Tan, A.R. Kuang, Y.C. Li, J.G. Zheng, W.M. Pan, [The radiolabeling property of oligonucleotide with 99mTc using NHS-MAG3 as a chelator]. Sichuan da xue xue bao Yi xue ban =, J. Sichuan Univ. Med. Sci. Ed. 35 (2004) 169–171.
[107] C. Van de Wiele, F. Dumont, R.A. Dierckx, S.H. Peers, J.R. Thornback, G. Slegers, et al., Biodistribution and dosimetry of (99m)Tc-RP527, a gastrin-releasing peptide (GRP) agonist for the visualization of GRP receptor-expressing malignancies, J. Nucl. Med. : Off. Publ. Soc. Nucl. Med. 42 (2001) 1722–1727.
[108] C. Van de Wiele, F. Dumont, R. Vanden Broecke, W. Oosterlinck, V. Cocquyt, R. Serreyn, et al., Technetium-99m RP527, a GRP analogue for visualisation of GRP receptor-expressing malignancies: a feasibility study, Eur. J. Nucl. Med. 27 (2000) 1694–1699.
[109] Y. Abe, N. Tanaka, The hedgehog signaling networks in lung cancer: the mechanisms and roles in tumor progression and implications for cancer therapy, BioMed Res. Int. 2016 (2016) 7969286.
[110] D.M. Berman, S.S. Karhadkar, A. Maitra, R. Montes De Oca, M.R. Gerstenblith, K. Briggs, et al., Widespread requirement for Hedgehog ligand stimulation in growth of digestive tract tumours, Nature 425 (2003) 846–851.
[111] M. Kubo, M. Nakamura, A. Tasaki, N. Yamanaka, H. Nakashima, M. Nomura, et al., Hedgehog signaling pathway is a new therapeutic target for patients with breast cancer, Cancer Res. 64 (2004) 6071–6074.
[112] T. Monkkonen, M.T. Lewis, New paradigms for the Hedgehog signaling network in mammary gland development and breast Cancer, Biochim. Biophys. Acta Rev. Canc. 1868 (2017) 315–332.
[113] S.P. Thayer, M.P. di Magliano, P.W. Heiser, C.M. Nielsen, D.J. Roberts, G.Y. Lauwers, et al., Hedgehog is an early and late mediator of pancreatic cancer tumorigenesis, Nature 425 (2003) 851–856.
[114] C. Wu, X. Zhu, W. Liu, T. Ruan, K. Tao, Hedgehog signaling pathway in colorectal cancer: function, mechanism, and therapy, OncoTargets Ther. 10 (2017) 3249–3259.
[115] K. Yanai, S. Nagai, J. Wada, N. Yamanaka, M. Nakamura, N. Torata, et al., Hedgehog signaling pathway is a possible therapeutic target for gastric cancer, J. Surg. Oncol. 95 (2007) 55–62.
[116] J. Sims-Mourtada, D. Yang, I. Tworowska, R. Larson, D. Smith, N. Tsao, et al., Detection of canonical hedgehog signaling in breast cancer by 131-iodine-labeled derivatives of the sonic hedgehog protein, J. Biomed. Biotechnol. 2012 (2012) 639562.
[117] M. Nakamura, M. Kubo, K. Yanai, Y. Mikami, M. Ikebe, S. Nagai, et al., Anti-patched-1 antibodies suppress hedgehog signaling pathway and pancreatic cancer proliferation, Anticancer Res. 27 (2007) 3743–3747.
[118] L.V. Goodrich, R.L. Johnson, L. Milenkovic, J.A. McMahon, M.P. Scott, Conservation of the hedgehog/patched signaling pathway from flies to mice: induction of a mouse patched gene by Hedgehog, Genes Dev. 10 (1996) 301–312.
[119] M. Nakamura, H. Tanaka, Y. Nagayoshi, H. Nakashima, K. Tsutsumi, T. Ohtsuka, et al., Targeting the hedgehog signaling pathway with interacting peptides to Patched-1, J. Gastroenterol. 47 (2012) 452–460.
[120] W. Campbell, L. Kleiman, L. Barany, Z. Li, A. Khorchid, E. Fujita, et al., A novel genetic algorithm for designing mimetic peptides that interfere with the function of a target molecule, Microbiol. Immunol. 46 (2002) 211–215.
[121] E. Pourbasheer, S. Ahmadpour, R. Zare-Dorabei, M. Nekoei, Quantitative structure activity relationship study of p38α MAP kinase inhibitors, Arabian J. Chem. 10 (2017) 33–40.
[122] D. Smith, F. Kong, D. Yang, R. Larson, J. Sims-Mourtada, W.A. Woodward, Patched targeting peptides for imaging and treatment of hedgehog positive breast tumors, BioMed Res. Int. 2014 (2014) 525680.
[123] F. Chai, J. Zhou, C. Chen, S. Xie, X. Chen, P. Su, et al., The Hedgehog inhibitor cyclopamine antagonizes chemoresistance of breast cancer cells, OncoTargets Ther. 6 (2013) 1643–1647.
[124] J. Sims-Mourtada, J.G. Izzo, J. Ajani, K.S. Chao, Sonic Hedgehog promotes multiple drug resistance by regulation of drug transport, Oncogene 26 (2007) 5674–5679.
[125] J. Sims-Mourtada, J.G. Izzo, S. Apisarnthanarax, T.T. Wu, U. Malhotra, R. Luthra, et al., Hedgehog: an attribute to tumor regrowth after chemoradiotherapy and a target to improve radiation response, Clin. Cancer Res. : Off. J. Am. Assoc. Canc. Res. 12 (2006) 6565–6572.
[126] S. Liu, G. Dontu, I.D. Mantle, S. Patel, N.S. Ahn, K.W. Jackson, et al., Hedgehog signaling and Bmi-1 regulate self-renewal of normal and malignant human mammary stem cells, Cancer Res. 66 (2006) 6063–6071.
[127] A. Berezov, J. Chen, Q. Liu, H.T. Zhang, M.I. Greene, R. Murali, Disabling receptor ensembles with rationally designed interface peptidomimetics, J. Biol. Chem. 277 (2002) 28330–28339.
[128] T. Engfeldt, A. Orlova, T. Tran, A. Bruskin, C. Widstrom, A.E. Karlstrom, et al., Imaging of HER2-expressing tumours using a synthetic Affibody molecule containing the 99mTc-chelating mercaptoacetyl-glycyl-glycyl-glycyl (MAG3) sequence, Eur. J. Nucl. Med. Mol. Imaging 34 (2007) 722–733.
[129] L. Geng, Z. Wang, X. Yang, D. Li, W. Lian, Z. Xiang, et al., Structure-based design of peptides with high affinity and specificity to HER2 positive tumors, Theranostics 5 (2015) 1154–1165.
[130] M.Z. Zhang, Y.X. Guan, J.X. Zhong, X.Z. Chen, Preparation and identification of HER2 radioactive ligands and imaging study of breast cancer-bearing nude mice, Transl. Oncol. 10 (2017) 518–526.
[131] N.G. Karasseva, V.V. Glinsky, N.X. Chen, R. Komatireddy, T.P. Quinn, Identification and characterization of peptides that bind human ErbB-2 selected from a bacteriophage display library, J. Protein Chem. 21 (2002) 287–296.

[132] S.R. Kumar, T.P. Quinn, S.L. Deutscher, Evaluation of an 111In-radiolabeled peptide as a targeting and imaging agent for ErbB-2 receptor expressing breast carcinomas, Clin. Cancer Res. : Off. J. Am. Assoc. Canc. Res. 13 (2007) 6070–6079.
[133] J. Folkman, Tumor angiogenesis: therapeutic implications, N. Engl. J. Med. 285 (1971) 1182–1186.
[134] F. Shojaei, Anti-angiogenesis therapy in cancer: current challenges and future perspectives, Cancer Lett. 320 (2012) 130–137.
[135] S.M. Chim, A. Qin, J. Tickner, N. Pavlos, T. Davey, H. Wang, et al., EGFL6 promotes endothelial cell migration and angiogenesis through the activation of extracellular signal-regulated kinase, J. Biol. Chem. 286 (2011) 22035–22046.
[136] G. Yeung, J.J. Mulero, R.P. Berntsen, D.B. Loeb, R. Drmanac, J.E. Ford, Cloning of a novel epidermal growth factor repeat containing gene EGFL6: expressed in tumor and fetal tissues, Genomics 62 (1999) 304–307.
[137] B.M. Larimer, W.D. Thomas, G.P. Smith, S.L. Deutscher, Affinity maturation of an ERBB2-targeted SPECT imaging peptide by in vivo phage display, Mol. Imag. Biol. Mib Off. Publ. Acad. Mol. Imag. 16 (2014) 449–458.
[138] B.M. Larimer, S.L. Deutscher, Development of a peptide by phage display for SPECT imaging of resistance-susceptible breast cancer, Am. J. Nucl. Med. Mol. Imag. 4 (2014) 435–447.
[139] E. Ruoslahti, RGD and other recognition sequences for integrins, Annu. Rev. Cell Dev. Biol. 12 (1996) 697–715.
[140] S.H. Barondes, D.N. Cooper, M.A. Gitt, H. Leffler, Galectins. Structure and function of a large family of animal lectins, J. Biol. Chem. 269 (1994) 20807–20810.
[141] H. Idikio, Galectin-3 expression in human breast carcinoma: correlation with cancer histologic grade, Int. J. Oncol. 12 (1998) 1287–1290.
[142] S. Morris, N. Ahmad, S. Andre, H. Kaltner, H.J. Gabius, M. Brenowitz, et al., Quaternary solution structures of galectins-1, -3, and -7, Glycobiology 14 (2004) 293–300.
[143] J. Ochieng, P. Warfield, B. Green-Jarvis, I. Fentie, Galectin-3 regulates the adhesive interaction between breast carcinoma cells and elastin, J. Cell. Biochem. 75 (1999) 505–514.
[144] A. Raz, R. Lotan, Endogenous galactoside-binding lectins: a new class of functional tumor cell surface molecules related to metastasis, Cancer Metastasis Rev. 6 (1987) 433–452.
[145] S. Akahani, P. Nangia-Makker, H. Inohara, H.R. Kim, A. Raz, Galectin-3: a novel antiapoptotic molecule with a functional BH1 (NWGR) domain of Bcl-2 family, Cancer Res. 57 (1997) 5272–5276.
[146] T. Fukumori, N. Oka, Y. Takenaka, P. Nangia-Makker, E. Elsamman, T. Kasai, et al., Galectin-3 regulates mitochondrial stability and antiapoptotic function in response to anticancer drug in prostate cancer, Cancer Res. 66 (2006) 3114–3119.
[147] H.C. Gong, Y. Honjo, P. Nangia-Makker, V. Hogan, N. Mazurak, R.S. Bresalier, et al., The NH2 terminus of galectin-3 governs cellular compartmentalization and functions in cancer cells, Cancer Res. 59 (1999) 6239–6245.
[148] H. Inohara, A. Raz, Functional evidence that cell surface galectin-3 mediates homotypic cell adhesion, Cancer Res. 55 (1995) 3267–3271.
[149] P. Matarrese, O. Fusco, N. Tinari, C. Natoli, F.T. Liu, M.L. Semeraro, et al., Galectin-3 overexpression protects from apoptosis by improving cell adhesion properties, Int. J. Cancer 85 (2000) 545–554.
[150] P. Nangia-Makker, Y. Honjo, R. Sarvis, S. Akahani, V. Hogan, K.J. Pienta, et al., Galectin-3 induces endothelial cell morphogenesis and angiogenesis, Am. J. Pathol. 156 (2000) 899–909.
[151] J. Zou, V.V. Glinsky, L.A. Landon, L. Matthews, S.L. Deutscher, Peptides specific to the galectin-3 carbohydrate recognition domain inhibit metastasis-associated cancer cell adhesion, Carcinogenesis 26 (2005) 309–318.
[152] V.V. Glinsky, G.V. Glinsky, K. Rittenhouse-Olson, M.E. Huflejt, O.V. Glinskii, S.L. Deutscher, et al., The role of Thomsen-Friedenreich antigen in adhesion of human breast and prostate cancer cells to the endothelium, Cancer Res. 61 (2001) 4851–4857.
[153] S.K. Khaldoyanidi, V.V. Glinsky, L. Sikora, A.B. Glinskii, V.V. Mossine, T.P. Quinn, et al., MDA-MB-435 human breast carcinoma cell homo- and heterotypic adhesion under flow conditions is mediated in part by Thomsen-Friedenreich antigen-galectin-3 interactions, J. Biol. Chem. 278 (2003) 4127–4134.
[154] S.R. Kumar, S.L. Deutscher, 111In-labeled galectin-3-targeting peptide as a SPECT agent for imaging breast tumors, J. Nucl. Med. : Off. Publ. Soc. Nucl. Med. 49 (2008) 796–803.
[155] E. Maquoi, D. Assent, J. Detilleux, C. Pequeux, J.M. Foidart, A. Noel, MT1-MMP protects breast carcinoma cells against type I collagen-induced apoptosis, Oncogene 31 (2012) 480–493.
[156] M. Seiki, Membrane-type 1 matrix metalloproteinase: a key enzyme for tumor invasion, Cancer Lett. 194 (2003) 1–11.
[157] M. Seiki, N. Koshikawa, I. Yana, Role of pericellular proteolysis by membrane-type 1 matrix metalloproteinase in cancer invasion and angiogenesis, Cancer Metastasis Rev. 22 (2003) 129–143.
[158] W.G. Jiang, G. Davies, T.A. Martin, C. Parr, G. Watkins, M.D. Mason, et al., Expression of membrane type-1 matrix metalloproteinase, MT1-MMP in human breast cancer and its impact on invasiveness of breast cancer cells, Int. J. Mol. Med. 17 (2006) 583–590.
[159] P. Laudanski, J. Swiatecka, L. Kozlowski, M. Lesniewska, M. Wojtukiewicz, S. Wolczynski, Increased serum level of membrane type 1-matrix metalloproteinase (MT1-MMP/MMP-14) in patients with breast cancer, Folia Histochem. Cytobiol. 48 (2010) 101–103.
[160] L. Zhu, H. Wang, L. Wang, Y. Wang, K. Jiang, C. Li, et al., High-affinity peptide against MT1-MMP for in vivo tumor imaging, J. Control. Release : Off. J. Control. Release Soc. 150 (2011) 248–255.
[161] K. Min, B. Ji, M. Zhao, T. Ji, B. Chen, X. Fang, et al., Development of a radiolabeled peptide-based probe targeting MT1-MMP for breast cancer detection, PLoS One 10 (2015) e0139471.
[162] S. Zitzmann, S. Kramer, W. Mier, U. Hebling, A. Altmann, A. Rother, et al., Identification and evaluation of a new tumor cell-binding peptide, FROP-1, J. Nucl. Med. : Off. Publ. Soc. Nucl. Med. 48 (2007) 965–972.
[163] W. Mier, S. Zitzmann, S. Kramer, J. Reed, E.M. Knapp, A. Altmann, et al., Influence of chelate conjugation on a newly identified tumor-targeting peptide, J. Nucl. Med. : Off. Publ. Soc. Nucl. Med. 48 (2007) 1545–1552.
[164] W. Mier, S. Kramer, S. Zitzmann, A. Altmann, K. Leotta, U. Schierbaum, et al., PEGylation enables the specific tumor accumulation of a peptide identified by phage display, Org. Biomol. Chem. 11 (2013) 2706–2711.
[165] J.M. Breuss, J. Gallo, H.M. DeLisser, I.V. Klimanskaya, H.G. Folkesson, J.F. Pittet, et al., Expression of the beta 6 integrin subunit in development, neoplasia and tissue repair suggests a role in epithelial remodeling, J. Cell Sci. 108 (Pt 6) (1995) 2241–2251.
[166] L. Hakkinen, L. Koivisto, H. Gardner, U. Saarialho-Kere, J.M. Carroll, M. Lakso, et al., Increased expression of beta6-integrin in skin leads to spontaneous development of chronic wounds, Am. J. Pathol. 164 (2004) 229–242.
[167] L.A. Van Aarsen, D.R. Leone, S. Ho, B.M. Dolinski, P.E. McCoon, D.J. LePage, et al., Antibody-mediated blockade of integrin alpha v beta 6 inhibits tumor progression in vivo by a transforming growth factor-beta-regulated mechanism, Cancer Res. 68 (2008) 561–570.
[168] R.C. Bates, D.I. Bellovin, C. Brown, E. Maynard, B. Wu, H. Kawakatsu, et al., Transcriptional activation of integrin beta6 during the epithelial-mesenchymal transition defines a novel prognostic indicator of aggressive colon carcinoma, J. Clin. Investig. 115 (2005) 339–347.
[169] A.N. Elayadi, K.N. Samli, L. Prudkin, Y.H. Liu, A. Bian, X.J. Xie, et al., A peptide selected by biopanning identifies the integrin alphavbeta6 as a prognostic biomarker for nonsmall cell lung cancer, Cancer Res. 67 (2007) 5889–5895.
[170] S. Hazelbag, G.G. Kenter, A. Gorter, E.J. Dreef, L.A. Koopman, S.M. Violette, et al., Overexpression of the alpha v beta 6 integrin in cervical squamous cell carcinoma is a prognostic factor for decreased survival, J. Pathol. 212 (2007) 316–324.
[171] J. Niu, X. Gu, J. Turton, C. Meldrum, E.W. Howard, M. Agrez, Integrin-mediated signalling of gelatinase B secretion in colon cancer cells, Biochem. Biophys. Res. Commun. 249 (1998) 287–291.
[172] G.J. Thomas, M.P. Lewis, S.A. Whawell, A. Russell, D. Sheppard, I.R. Hart, et al., Expression of the alphavbeta6 integrin promotes migration and invasion in squamous carcinoma cells, J. Investig. Dermatol. 117 (2001) 67–73.
[173] G.J. Thomas, M.L. Nystrom, J.F. Marshall, Alphavbeta6 integrin in wound healing and cancer of the oral cavity, J. Oral Pathol. Med. : Off. Publ. Int. Assoc. Oral Pathol. Am. Acad. Oral Pathol. 35 (2006) 1–10.
[174] D. DiCara, C. Rapisarda, J.L. Sutcliffe, S.M. Violette, P.H. Weinreb, I.R. Hart, et al., Structure-function analysis of Arg-Gly-Asp helix motifs in alpha v beta 6 integrin ligands, J. Biol. Chem. 282 (2007) 9657–9665.
[175] A. Saha, D. Ellison, G.J. Thomas, S. Vallath, S.J. Mather, I.R. Hart, et al., High-resolution in vivo imaging of breast cancer by targeting the pro-invasive integrin alphavbeta6, J. Pathol. 222 (2010) 52–63.
[176] S.H. Hausner, D. DiCara, J. Marik, J.F. Marshall, J.L. Sutcliffe, Use of a peptide derived from foot-and-mouth disease virus for the noninvasive imaging of human cancer: generation and evaluation of 4-[18F]fluorobenzoyl A20FMDV2 for in vivo imaging of integrin alphavbeta6 expression with positron emission tomography, Cancer Res. 67 (2007) 7833–7840.
[177] S.J. Santner, P.J. Dawson, L. Tait, H.D. Soule, J. Eliason, A.N. Mohamed, et al., Malignant MCF10CA1 cell lines derived from premalignant human breast epithelial MCF10AT cells, Breast Canc. Res. Treat. 65 (2001) 101–110.
[178] G. Fuh, K.C. Garcia, A.M. de Vos, The interaction of neuropilin-1 with vascular endothelial growth factor and its receptor flt-1, J. Biol. Chem. 275 (2000) 26690–26695.
[179] A.L. Kolodkin, D.V. Levengood, E.G. Rowe, Y.T. Tai, R.J. Giger, D.D. Ginty, Neuropilin is a semaphorin III receptor, Cell 90 (1997) 753–762.
[180] S. Soker, S. Takashima, H.Q. Miao, G. Neufeld, M. Klagsbrun, Neuropilin-1 is expressed by endothelial and tumor cells as an isoform-specific receptor for vascular endothelial growth factor, Cell 92 (1998) 735–745.
[181] L.M. Ellis, The role of neuropilins in cancer, Mol. Cancer Ther. 5 (2006) 1099–1107.
[182] S. Ghosh, C.A. Sullivan, M.P. Zerkowski, A.M. Molinaro, D.L. Rimm, R.L. Camp, et al., High levels of vascular endothelial growth factor and its receptors (VEGFR-1, VEGFR-2, neuropilin-1) are associated with worse outcome in breast cancer, Hum. Pathol. 39 (2008) 1835–1843.
[183] G.J. Prud'homme, Y. Glinka, Neuropilins are multifunctional coreceptors involved in tumor initiation, growth, metastasis and immunity, Oncotarget 3 (2012) 921–939.
[184] T.M. Hong, Y.L. Chen, Y.Y. Wu, A. Yuan, Y.C. Chao, Y.C. Chung, et al., Targeting neuropilin 1 as an antitumor strategy in lung cancer, Clin. Cancer Res. 13 (2007) 4759–4768.
[185] A. Starzec, R. Vassy, A. Martin, M. Lecouvey, M. Di Benedetto, M. Crepin, et al., Antiangiogenic and antitumor activities of peptide inhibiting the vascular endothelial growth factor binding to neuropilin-1, Life Sci. 79 (2006) 2370–2381.
[186] T. Teesalu, K.N. Sugahara, V.R. Kotamraju, E. Ruoslahti, C-end rule peptides mediate neuropilin-1-dependent cell, vascular, and tissue penetration, Proc. Natl. Acad. Sci. U. S. A. 106 (2009) 16157–16162.
[187] G.K. Feng, R.B. Liu, M.Q. Zhang, X.X. Ye, Q. Zhong, Y.F. Xia, et al., SPECT and near-infrared fluorescence imaging of breast cancer with a neuropilin-1-targeting peptide, J. Control. Release : Off. J. Control. Release Soc. 192 (2014) 236–242.
[188] K.N. Sugahara, T. Teesalu, P.P. Karmali, V.R. Kotamraju, L. Agemy, O.M. Girard, et al., Tissue-penetrating delivery of compounds and nanoparticles into tumors, Cancer Cell 16 (2009) 510–520.

[189] E. Calce, L. Monfregola, A. Sandomenico, M. Saviano, S. De Luca, Fluorescence study for selecting specific ligands toward HER2 receptor: an example of receptor fragment approach, Eur. J. Med. Chem. 61 (2013) 116–121.
[190] E. Calce, A. Sandomenico, M. Saviano, M. Ruvo, S. De Luca, Cysteine co-oxidation process driven by native peptide folding: an example on HER2 receptor model system, Amino Acids 46 (2014) 1197–1206.
[191] L. Monfregola, R.M. Vitale, P. Amodeo, S. De Luca, A SPR strategy for high-throughput ligand screenings based on synthetic peptides mimicking a selected subdomain of the target protein: a proof of concept on HER2 receptor, Bioorg. Med. Chem. 17 (2009) 7015–7020.
[192] H. Honarvar, E. Calce, N. Doti, E. Langella, A. Orlova, J. Buijs, et al., Evaluation of HER2-specific peptide ligand for its employment as radiolabeled imaging probe, Sci. Rep. 8 (2018) 2998.
[193] V. Tolmachev, T.A. Tran, D. Rosik, A. Sjoberg, L. Abrahmsen, A. Orlova, Tumor targeting using affibody molecules: interplay of affinity, target expression level, and binding site composition, J. Nucl. Med. : Off. Publ. Soc. Nucl. Med. 53 (2012) 953–960.
[194] P. Barta, J. Malmberg, L. Melicharova, J. Strandgard, A. Orlova, V. Tolmachev, et al., Protein interactions with HER-family receptors can have different characteristics depending on the hosting cell line, Int. J. Oncol. 40 (2012) 1677–1682.
[195] V. Askoxylakis, W. Mier, S. Zitzmann, V. Ehemann, J. Zhang, S. Kramer, et al., Characterization and development of a peptide (p160) with affinity for neuroblastoma cells, J. Nucl. Med. 47 (2006) 981–988.
[196] J. Zhang, H. Spring, M. Schwab, Neuroblastoma tumor cell-binding peptides identified through random peptide phage display, Cancer Lett. 171 (2001) 153–164.
[197] V. Askoxylakis, S. Zitzmann, W. Mier, K. Graham, S. Kramer, F. von Wegner, et al., Preclinical evaluation of the breast cancer cell-binding peptide, p160, Clin. Cancer Res. : Off. J. Am. Assoc. Canc. Res. 11 (2005) 6705–6712.
[198] M. Shahin, R. Soudy, H.M. Aliabadi, N. Kneteman, K. Kaur, A. Lavasanifar, Engineered breast tumor targeting peptide ligand modified liposomal doxorubicin and the effect of peptide density on anticancer activity, Biomaterials 34 (2013) 4089–4097.
[199] R. Soudy, C. Chen, K. Kaur, Novel peptide-doxorubucin conjugates for targeting breast cancer cells including the multidrug resistant cells, J. Med. Chem. 56 (2013) 7564–7573.
[200] R. Soudy, H. Etayash, K. Bahadorani, A. Lavasanifar, K. Kaur, Breast cancer targeting peptide binds keratin 1: a new molecular marker for targeted drug delivery to breast cancer, Mol. Pharm. 14 (2017) 593–604.
[201] V. Blanckaert, V. Kerviel, A. Lepinay, V. Joubert-Durigneux, H. Hondermarck, B. Chenais, Docosahexaenoic acid inhibits the invasion of MDA-MB-231 breast cancer cells through upregulation of cytokeratin-1, Int. J. Oncol. 46 (2015) 2649–2655.
[202] J.T. DeAngelis, Y. Li, N. Mitchell, L. Wilson, H. Kim, T.O. Tollefsbol, 2D difference gel electrophoresis analysis of different time points during the course of neoplastic transformation of human mammary epithelial cells, J. Proteome Res. 10 (2011) 447–458.
[203] V. Karantza, Keratins in health and cancer: more than mere epithelial cell markers, Oncogene 30 (2011) 127–138.
[204] D.K. Trask, V. Band, D.A. Zajchowski, P. Yaswen, T. Suh, R. Sager, Keratins as markers that distinguish normal and tumor-derived mammary epithelial cells, Proc. Natl. Acad. Sci. U. S. A. 87 (1990) 2319–2323.